Nonstationary shot noise modeling of neuron membrane potentials by closed-form moments and Gram-Charlier expansions

Nicolas Privault*
Division of Mathematical Sciences
School of Physical and Mathematical Sciences
Nanyang Technological University
21 Nanyang Link
Singapore 637371

October 3, 2020

Abstract

We present exact analytical expressions of moments of all orders for neuronal membrane potentials in the multiplicative nonstationary Poisson shot noise model. As an application, we derive closed-form Gram-Charlier density expansions that show how the probability density functions of potentials in such models differ from their Gaussian diffusion approximations. This approach extends the results of Brigham and Destexhe (2015a;b) by the use of exact combinatorial expressions for the moments of multiplicative nonstationary filtered shot noise processes. Our results are confirmed by stochastic simulations, and apply to single and multiple noise source models.

Key words: Filtered shot noise processes; Poisson point processes; moments; cumulants; Gram-Charlier expansions; conductance synapses; membrane potentials.

1 Introduction

Neuronal synaptic input can be modeled using multiplicative shot noise driven by random conductance spikes, see for example Verveen and DeFelice (1974), Tuckwell (1988) for the use of filtered Poisson shot noise. In the case of constant Poisson arrival

*nprivault@ntu.edu.sg

rates, the stationary limit of those systems has been analyzed in Kuhn et al. (2004), Rudolph and Destexhe (2005), Richardson and Gerstner (2005), Burkitt (2006a), via approximations formulas. In Wolff and Lindner (2008; 2010), exact analytical expressions for the time-dependent mean and standard deviation of membrane potentials have been derived in filtered Poisson shot noise models.

Poisson shot noise processes with time-dependent intensities have been used for the modeling of time-inhomogeneous synaptic input in e.g. Amemori and Ishii (2001), Burkitt (2006b), Cai et al. (2006). In this framework, the time evolution of the probability density functions of membrane potentials has been modeled by Gram-Charlier density expansions based on moment and cumulant estimates in Brigham and Destexhe (2015a;b). It has been observed in Brigham and Destexhe (2015a) that Gram-Charlier density expansions can provide a better fit of the actual densities generated by Monte Carlo simulations, in comparison to the Gaussian diffusion approximation. However, only the first and second cumulants have been computed explicitly in Brigham and Destexhe (2015a;b), while higher-order cumulants and moments have been approximated by other means such as Monte Carlo simulations.

In this paper, we present closed-form expressions of moments and cumulants of all orders for the solutions of first-order linear inhomogeneous Ordinary Differential Equations (ODEs) driven by Poisson shot noise processes. As a result, we are able to derive closed-form Gram-Charlier density expansions for the probability density functions of membrane potentials. We work in the multiple source model of Brigham and Destexhe (2015a), which is based on a Poisson point process ξ on $\mathbb{X} = \mathbb{R} \times [0, N]$ and N shot noise conductance processes $Q_k(t, \xi)$ representing the inputs of N conductance synapses. This paper can be regarded as a continuation of the moment computations of Brigham and Destexhe (2015a;b), based on iterations of the Slivnyak-Mecke formula (Slivnyak (1962), Mecke (1967)). Similar extensions to higher moments are possible by the method of Wolff and Lindner (2008), based on multiple differentiations of the Laplace transform of the integrated shot noise.

In Proposition 2.2 and Relation (2.6) we compute the joint moments of the membrane potentials $Y_N(t_1, \xi), \ldots, Y_N(t_n, \xi)$ modeled according to the filtered shot noise (2.1) below, with exact analytical expressions given for third and fourth moments

in Relations (3.3)-(3.4). Our results are based on closed-form moment identities for stochastic integrals of random integrands with respect to Poisson point processes which are stated in Proposition 5.6 in the appendix, see Privault (2009; 2012), and Privault (2016) for a review. In comparison with Monte Carlo simulation estimates, explicit expressions are suitable for algebraic manipulations and tabulation, e.g. they can be differentiated in closed form with respect to time to yield the dynamics of the cumulants, or with respect to any system parameter to yield sensitivity measures.

Those expressions are then applied in Section 3 to the explicit derivation of cumulant-based Gram-Charlier expansions for the probability density function of the membrane potentials $Y_N(t,\xi)$ at any time $t > 0$, with numerical simulations provided in Section 4 in single and double source models. The simulation results show significant differences, in particular in terms of skewness of densities, between the Poisson shot noise model and its Gaussian diffusion approximation, cf. Figures 9 and 20. Namely, densities appear negatively skewed with positive excess kurtosis in the single source model, and positively skewed with negative excess kurtosis in the nonstationary multiple source model which involves excitatory and inhibitory leak potentials of opposite signs, see Figure 23. We also note that higher-order cumulant estimates obtained by Monte Carlo simulations can be subject to numerical instabilities not observed with the closed-form expressions, see Figures 16-a,b), and 17-a) and 19. In addition, a single high-precision Monte Carlo simulation over a large number of samples can be slower than the numerical evaluation of the corresponding exact expression.

We proceed as follows. In Section 2 we review the construction of nonstationary filtered shot noise processes in the multiple source model of Brigham and Destexhe (2015a), followed by its single source specialization, see Brigham and Destexhe (2015b). We also discuss their diffusion approximation and a result on existence of probability densities. Exact expressions for the joint moments and cumulants of the potential $V_N(t)$ are then presented in Sections 3 and 4.1. In Section 4 we present numerical experiments based on cumulant-based Gram-Charlier expansions in the single source and double source models. Section 5 reviews the derivation of moment identities for the moments of Poisson stochastic integrals with random integrands, and

includes the technical proofs of Propositions 5.3 and 5.6.

2 Nonstationary multiplicative shot noise model

In this section we consider the multiple source model of Brigham and Destexhe (2015a), based on a Poisson point process $\xi(dx)$ on the space

$$\Omega := \big\{\xi = \{x_i\}_{i\in I} \subset \mathbb{X} \ : \ \#(A\cap\xi) < \infty \text{ for all compact } A \in \mathcal{B}(\mathbb{X})\big\}$$

of locally finite configurations with the intensity measure $\mu(dt, d\theta)$ on $\mathbb{X} = \mathbb{R}\times S$, where $S = [0, N]$. We consider N shot noise conductance processes

$$Q_k(t,\xi) = \int_{(-\infty,t]\times S} g_k(t-s,\theta)\xi(ds,d\theta) = \sum_{(s_j,\theta_j)\in\xi} g_k(t-s_j,\theta_j), \quad k = 1,\ldots,N,$$

which represent the inputs of N conductance synapses. The shot noise kernels $g_k(u,\theta)$ represent the impulse response functions and are such that $g_k(u,\theta) = 0$ for $u < 0$, where $g_k(t-s,\theta)$ represents the leak conductance, the s_j's are the presynaptic events, and the θ_j's are modeling possible synaptic inhomogeneities. In this framework, the moment generating function of the conductance process $Q_k(t,\xi)$ is known to be given by

$$\langle \exp\left(Q_k(t,\xi)\right)\rangle = \exp\left(\int_{(-\infty,t]\times S} (\mathrm{e}^{g_k(t-u,\theta)} - 1)\mu(du,d\theta)\right),$$

see the Lévy-Khintchine formula (5.2). The system response is modeled by the membrane potential $Y_N(t,\xi)$ satisfying the unit-less shot noise Stochastic Differential Equation (SDE)

$$\tau\frac{dY_N}{dt}(t,\xi) = -Y_N(t,\xi) + \sum_{k=1}^{N}(w_k - Y_N(t,\xi))Q_k(t,\xi), \tag{2.1}$$

where $\tau > 0$ is the membrane time constant and $w_k \in \mathbb{R}$, $k = 1,\ldots,N$, represent the (renormalized) leak potentials.

The solution of (2.1) is derived in the next proposition, which can be proved by standard calculations, see § 2.1 of Brigham and Destexhe (2015a).

Proposition 2.1 *The solution of* (2.1) *is given by the filtered shot noise process*

$$Y_N(t,\xi) = \frac{1}{\tau}\sum_{k=1}^{N} w_k \int_{-\infty}^{t} Q_k(z,\xi)\mathrm{e}^{-\int_z^t Q_0(u,\xi)du}dz, \qquad t\in\mathbb{R}, \tag{2.2}$$

where

$$Q_0(u,\xi) := \frac{1}{\tau} + \frac{1}{\tau}\sum_{k=1}^{N} Q_k(u,\xi).$$

Letting

$$f(z,\theta) := \sum_{k=1}^{N} g_k(z,\theta) \quad \text{and} \quad f^{(w)}(z,\theta) := \sum_{k=1}^{N} w_k g_k(z,\theta), \quad z \in \mathbb{R},\ \theta \in S,$$

we can also write

$$Q_0(t,\xi) = \frac{1}{\tau} + \frac{1}{\tau}\int_{(-\infty,t]\times S} f(t-s,\theta)\xi(ds,d\theta) = \frac{1}{\tau} + \frac{1}{\tau}\sum_{(s_j,\theta_j)\in\xi} f(t-s_j,\theta_j),$$

and

$$Y_N(t,\xi) = \frac{1}{\tau}\int_{-\infty}^{t} \mathrm{e}^{-\int_z^t Q_0(s,\xi)ds} \int_{(-\infty,z]\times S} f^{(w)}(z-s,\theta)\xi(ds,d\theta)dz. \tag{2.3}$$

Computation of joint moments

The next proposition gives a general formula for the computation of the joint moments of $Y_N(t_1,\xi),\ldots,Y_N(t_n,\xi)$ in the multiple source model as a direct consequence of (2.3).

Proposition 2.2 *We have the joint moment identity*

$$\langle Y_N(t_1,\xi)\cdots Y_N(t_n,\xi)\rangle = \frac{1}{\tau^n}\int_{-\infty}^{t_1}\cdots\int_{-\infty}^{t_n} m_{n,N}(z_1,\ldots,z_n;t_1,\ldots,t_n)dz_1\cdots dz_n, \tag{2.4}$$

where

$$m_{n,N}(z_1,\ldots,z_n;t_1,\ldots,t_n) := \left\langle \prod_{k=1}^{n}\left(\mathrm{e}^{-\int_{z_l}^{t_l} Q_0(u,\xi)du}\int_{(-\infty,z_k]\times S} f^{(w)}(z_k-u,\theta)\xi(du,d\theta)\right)\right\rangle. \tag{2.5}$$

By Proposition 5.6 in the appendix, the function $m_{n,N}(z_1,\ldots,z_n;t_1,\ldots,t_n)$ can be evaluated as a sum over the set $\Pi[n]$ of partitions $\pi=\{\pi_1,\ldots,\pi_k\}$ of $\{1,\ldots,n\}$ with cardinality $k=|\pi|=1,\ldots,n$, as

$$\begin{aligned} &m_{n,N}(z_1,\ldots,z_n;t_1,\ldots,t_n) \qquad (2.6)\\ &= \left\langle \mathrm{e}^{-\sum_{l=1}^{n}\int_{z_l}^{t_l} Q_0(u,\xi)du}\right\rangle \sum_{\pi\in\Pi[n]}\prod_{j=1}^{|\pi|}\int_{(-\infty,\hat{z}_{\pi_j}]\times S}\prod_{l=1}^{n}\mathrm{e}^{-\frac{1}{\tau}\int_{z_l}^{t_l} f(u-y,\eta)du}\prod_{i\in\pi_j} f^{(w)}(z_i-y,\eta)\mu(\mathrm{d}y,\mathrm{d}\eta), \end{aligned}$$

$(z_1,\dots,z_n)\in(-\infty,t_1]\times\cdots\times(-\infty,t_n]$, with $\hat{z}_{\pi_j}=\min_{i\in\pi_j}z_i$, where, by the Lévy-Khintchine formula (5.2),

$$\begin{aligned}&\left\langle \mathrm{e}^{-\sum_{l=1}^n\int_{z_l}^{t_l}Q_0(u,\xi)du}\right\rangle \\ &= \mathrm{e}^{-\frac{1}{\tau}\sum_{l=1}^n(t_l-z_l)}\exp\left(\int_{(-\infty,\max(t_1,\dots,t_n)]\times S}\left(\mathrm{e}^{-\frac{1}{\tau}\sum_{l=1}^n\int_{z_l}^{t_l}f(u-s,\theta)du}-1\right)\mu(ds,d\theta)\right).\end{aligned}\tag{2.7}$$

In the case of ordinary moments $\langle(Y_N(t,\xi))^n\rangle$, the function $m_{n,N}(z_1,\dots,z_n;t_1,\dots,t_n)$ is symmetric in $(z_1,\dots,z_n)$ hence we can replace the sum over partitions in (2.6) with the summation over integer compositions

$$\begin{aligned}&m_{n,N}(z_1,\dots,z_n;t,\dots,t)=\left\langle \mathrm{e}^{-\sum_{l=1}^n\int_{z_l}^{t}Q_0(u,\xi)du}\right\rangle \\ &\times\sum_{k=1}^n\sum_{\substack{l_1+\cdots+l_k=n\\ l_1\geq1,\dots,l_k\geq1}}\frac{n!}{k!l_1!\cdots l_k!}\prod_{j=1}^k\int_{(-\infty,\hat{z}_k]\times S}\prod_{l=1}^n\mathrm{e}^{-\frac{1}{\tau}\int_{z_l}^t f(u-y,\eta)du}\prod_{i=1+l_1+\cdots+l_{k-1}}^{l_1+\cdots+l_k}f^{(w)}(z_i-y,\eta)\mu(\mathrm{d}y,\mathrm{d}\eta)\end{aligned}\tag{2.8}$$

with $\hat{z}_k=\min_{l_1+\cdots+l_{k-1}<j\leq l_1+\cdots+l_k}z_j\in(-\infty,t]$, $k=1,\dots,n$. Explicit formulas for the first four moments of $Y_N(t,\xi)$ in the multiple source model (2.2) will be presented in Section 3 as a consequence of (2.8). Such formulas allow for the explicit computation of joint moment dynamics instead of solving the differential equation (2.9).

Dynamics of moments

The dynamics of moments $\langle(Y_N(t,\xi))^n\rangle$ of $Y_N(t,\xi)$ can be determined in terms of the joint moments $\langle(Y_N(t,\xi))^{n-1}Q_k(t,\xi)\rangle$, $\langle(Y_N(t,\xi))^nQ_k(t,\xi)\rangle$.

Proposition 2.3 *The moment $\langle(Y_N(t,\xi))^n\rangle$ of order $n\geq1$ of $Y_N(t,\xi)$ satisfy the differential equation*

$$\begin{aligned}\tau\frac{d\langle(Y_N(t,\xi))^n\rangle}{dt} &= -n\tau\langle(Y_N(t,\xi))^n\rangle \\ &\quad+n\sum_{k=1}^N w_k\langle(Y_N(t,\xi))^{n-1}Q_k(t,\xi)\rangle-n\sum_{k=1}^N\langle(Y_N(t,\xi))^nQ_k(t,\xi)\rangle.\end{aligned}\tag{2.9}$$

Proof. From (2.1), we have

$$\begin{aligned}\tau(Y_N(t,\xi))^n&=\tau(Y_N(0,\xi))^n+\tau\int_0^t d(Y_N(s,\xi))^n\\ &= \tau(Y_N(0,\xi))^n+n\tau\int_0^t(Y_N(s,\xi))^{n-1}dY_N(s,\xi)\end{aligned}$$

$$= \tau(Y_N(0,\xi))^n - n\tau \int_0^t (Y_N(s,\xi))^n ds$$
$$+n \sum_{k=1}^N w_k \int_0^t (Y_N(s,\xi))^{n-1} Q_k(s,\xi) ds - n \sum_{k=1}^N \int_0^t (Y_N(s,\xi))^n Q_k(s,\xi) ds.$$

We conclude by taking expectations on both sides of the above expression, and by differentiating with respect to t. □

The joint moments appearing in (2.9) can be computed using Corollary 5.5. Alternatively, the dynamics of moments can be derived by differentiating closed-form moment expressions (2.4) and (2.6) with respect to time.

Diffusion approximation

Our density estimates in Poisson shot noise models will be compared in the sequel to their Gaussian diffusion approximation. A classical method to derive a diffusion approximation for the evolution of membrane potentials, see e.g. Lánský and Lánská (1987), is to use a Gaussian diffusion process $Z_N(t)$ matching the first and second moments of $Y_N(t)$ at any time $t \geq 0$. For example, one can choose a mean-reverting SDE of the form

$$dZ_N(t) = (a(t) - b(t)Z_N(t))dt + \sigma(t)dW(t), \tag{2.10}$$

with respect to a standard Brownian motion $(W(t))_{t\in\mathrm{R}_+}$, with solution

$$Z_N(t) = Z_N(0)\mathrm{e}^{-\int_0^t b(s)ds} + \int_0^t a(s)\mathrm{e}^{-\int_s^t b(u)du} ds + \int_0^t \sigma(s)\mathrm{e}^{-\int_s^t b(u)du} dW(s),$$

and moments of first and second order given by

$$\langle Z_N(t)\rangle = Z_N(0)\mathrm{e}^{-\int_0^t b(s)ds} + \int_0^t a(s)\mathrm{e}^{-\int_s^t b(u)du} ds, \tag{2.11}$$

and

$$\langle (Z_N(t) - \langle Z_N(t)\rangle)^2\rangle = \int_0^t \sigma^2(s)\mathrm{e}^{-2\int_s^t b(u)du} ds. \tag{2.12}$$

The diffusion approximation of $(Y_N(t))_{t\in\mathrm{R}_+}$ by $(Z_N(t))_{t\in\mathrm{R}_+}$ can then be constructed by identifying the coefficients $a(t)$, $b(t)$ and $\sigma(t)$ after matching (2.11)-(2.12) to the first and second moments of $Y_N(t)$, $t \in \mathbb{R}_+$.

Single source shot noise model

Before proceeding to the computation of moments in the multiple source case, we make some comments on the single source case with $N = 1$. We have $f^{(w)}(z, \theta) := w_1 g_1(z, \theta)$, $f(z, \theta) = g_1(z, \theta)$, $z \in \mathbb{R}$, $\theta \in S$, and

$$Y_1(t, \xi) = \frac{w_1}{\tau} \int_{-\infty}^{t} Q_1(z, \xi) \mathrm{e}^{-\int_z^t Q_0(u,\xi)du} dz,$$

with

$$Q_0(u, \xi) := \frac{1}{\tau} + \frac{1}{\tau} Q_1(u, \xi) = \frac{1}{\tau} + \frac{1}{\tau} \int_{(-\infty,u]\times S} g_1(u - s, \theta)\xi(ds, d\theta).$$

In this case, the membrane potential

$$Y_1(t, \xi) = \frac{1}{\tau} \int_{-\infty}^{t} Q_1(z, \xi) \exp\left(- \int_z^t Q_0(u, \xi)du \right) dz, \tag{2.13}$$

solution of (2.1) for $N = 1$ can be rewritten by integration by parts on $(-\infty, t]$ as

$$Y_1(t, \xi) = 1 - \frac{1}{\tau} \int_{-\infty}^{t} \exp\left(- \int_z^t Q_0(u, \xi)du \right) dz \tag{2.14}$$

with $Q_0(u, \xi) := 1/\tau + Q_1(u, \xi)/\tau$, see Relation (4) in Brigham and Destexhe (2015b). Figure 1 presents random simulations of the shot noise process $Q_1(t, \xi)$ and membrane potential $Y_1(t, \xi)$ in the unit-less single source model (2.13) with the parameters of Brigham and Destexhe (2015b), i.e. $N = 1$, $\mathbb{X} = \mathbb{R} \times \{0\}$, $\mu(dt) = \mathbb{1}_{[0,\infty)}(t)\lambda(t)dt$, plotted together with the intensity $\lambda(t) := \lambda \mathbf{1}_{[t_a,t_b]}(t)$, see also Figure 1 therein. Here, we take $T = 0.1s$, $w_1 = 1$ and $g_1(u) = h\mathrm{e}^{-u/\tau_s} \mathbf{1}_{[0,\infty)}(u)$, with $t_a = 0.01$s, $t_b = 0.05$s, $\tau = 0.02$s, $\lambda = 500$Hz, $h = 2$, and $\tau_s = 0.0025$s.

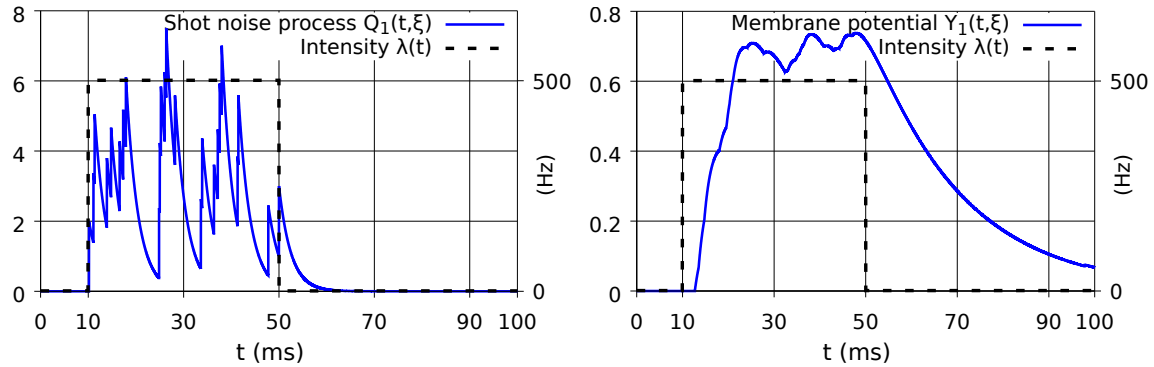

(a) Shot noise process $Q_1(t, \xi)$. (b) Membrane potential $Y_1(t, \xi)$.

Figure 1: Filtered shot noise processes and intensity function $\lambda(t) = \lambda \mathbf{1}_{[t_a,t_b]}(t)$.

Defining

$$\begin{aligned} Z(t,\xi) &:= \int_{-\infty}^{t} \exp\left(-\int_{z}^{t} Q_0(u,\xi)du\right) dz \\ &= \int_{-\infty}^{t} \exp\left(-\frac{t-z}{\tau} - \frac{1}{\tau}\int_{z}^{t} Q_1(u,\xi)du\right) dz, \end{aligned}$$

the moments of

$$Y_1(t,\xi) = 1 - \frac{1}{\tau} Z(t,\xi) \tag{2.15}$$

can then be computed from the moments of $Z(t,\xi)$. Relation (2.15) can be used to estimate all joint moments of $Y_1(t,\xi)$ in (2.14) and to recover its joint cumulants from (4.1) as in Relation (13) of Brigham and Destexhe (2015b), based on the joint moments of $Z(t_1,\xi),\ldots,Z(t_n,\xi)$ given from the Lévy-Khintchine formula (5.2) as

$$\begin{aligned} &\langle Z(t_1,\xi)\cdots Z(t_n,\xi)\rangle \\ &= \int_{-\infty}^{t_1}\cdots\int_{-\infty}^{t_n} \left\langle \prod_{i=1}^{n} \mathrm{e}^{-\int_{z_i}^{t_i} Q_0(u,\xi)du} \right\rangle dz_1\cdots dz_n \\ &= \int_{-\infty}^{t_1}\cdots\int_{-\infty}^{t_n} \exp\left(-\frac{1}{\tau}\sum_{l=1}^{n}(t_l - z_l) + \int_{\mathbb{X}} \left(\mathrm{e}^{-\frac{1}{\tau}\sum_{i=1}^{n}\int_{z_i}^{t_i} g_1(u-x,\theta)du} - 1\right)\mu(dx,d\theta)\right) dz_1\cdots dz_n, \end{aligned}$$

see Relation (13) in Brigham and Destexhe (2015b). For $n=1$ this yields

$$\begin{aligned} \langle Y_1(t,\xi)\rangle &= 1 - \frac{1}{\tau}\langle Z(t,\xi)\rangle \\ &= 1 - \frac{1}{\tau}\int_{-\infty}^{t} \mathrm{e}^{-(t-z)/\tau} \exp\left(\int_{(-\infty,t]\times S} \left(\mathrm{e}^{-\frac{1}{\tau}\int_{z}^{t} g_1(u-x,\theta)du} - 1\right)\mu(dx,d\theta)\right) dz, \end{aligned}$$

see Equation (12) in Brigham and Destexhe (2015b). However, estimating the expression (2.14) requires to integrate over x in $(-\infty,t]$, which appears to be more demanding from a numerical point of view. In addition, the integration by parts method that leads to (2.14) is only available in the case of $N=1$ source. For this reason, in Section 3 we develop a different approach to the computation of moments in both the multiple and single source models (2.2) and (2.13), by only using integrals of continuous bounded functions on compact intervals.

3 Joint moments of Poisson shot noise SDEs

In this section, we present the computation of the first four moments of $Y_N(t,\xi)$ in the multiple source model, based on the results of Section 5. We start with the first two

moments, in which case our results coincide with Brigham and Destexhe (2015a;b).

First moment

When $n = 1$ we have $\pi_1 = \{1\}$, hence by (2.4) the moment $\langle Y_N(t_1, \xi)\rangle$ can be computed from

$$m_{1,N}(z_1, t_1) = \left\langle \mathrm{e}^{-\int_{z_1}^{t_1} Q_0(u,\xi)du} \int_{(-\infty,z_1]\times S} f^{(w)}(z_1 - u, \theta)\xi(du, d\theta) \right\rangle \tag{3.1}$$

$$= \int_{-\infty}^{t_1} \left\langle \mathrm{e}^{-\int_{z_1}^{t_1} Q_0(u,\xi)du} \right\rangle \sum_{k=1}^{N} w_k \int_{(-\infty,z_1]\times S} \mathrm{e}^{-\frac{1}{\tau}\int_{z_1}^{t_1} g_k(u-y,\eta)du} g_k(z_1 - y, \eta)\mu(\mathrm{d}y, \mathrm{d}\eta)dz_1,$$

see Equations (6) and (8) page 3 of Brigham and Destexhe (2015b), and Equation (19) page 8 of Brigham and Destexhe (2015a).

Second joint moment

When $n = 2$ the two partitions of $\{1, 2\}$ can be listed as $\pi_1 =$ '12', and $\pi_1|\pi_2 =$ '1|2', hence by (2.4) the joint moment $\langle Y_N(t_1, \xi)Y_N(t_2, \xi)\rangle$ can be computed from

$$\begin{aligned}
&m_{2,N}(z_1, z_2; t_1, t_2) \\
&= \left\langle \mathrm{e}^{-\int_{z_1}^{t_1} Q_0(u,\xi)du - \int_{z_2}^{t_2} Q_0(u,\xi)du} \int_{(-\infty,z_1]\times S} f^{(w)}(z_1 - u, \theta)\xi(du, d\theta) \int_{(-\infty,z_2]\times S} f^{(w)}(z_2 - u, \theta)\xi(du, d\theta) \right\rangle \\
&= \left\langle \mathrm{e}^{-\int_{z_1}^{t_1} Q_0(u,\xi)du - \int_{z_2}^{t_2} Q_0(u,\xi)du} \right\rangle \\
&\quad \times \left(\int_{(-\infty,\min(z_1,z_2)]\times S} \mathrm{e}^{-\frac{1}{\tau}\int_{z_1}^{t_1} f(u-y,\eta)du - \frac{1}{\tau}\int_{z_2}^{t_2} f(u-y,\eta)du} f^{(w)}(z_1 - y, \eta) f^{(w)}(z_2 - y, \eta)\mu(\mathrm{d}y, \mathrm{d}\eta) \right. \\
&\quad + \int_{(-\infty,z_1]\times S} \mathrm{e}^{-\frac{1}{\tau}\sum_{l=1}^{2}\int_{z_l}^{t_l} f(u-y,\eta)du} f^{(w)}(z_1 - y, \eta)\mu(\mathrm{d}y, \mathrm{d}\eta) \\
&\quad \left. \times \int_{(-\infty,z_2]\times S} \mathrm{e}^{-\frac{1}{\tau}\sum_{l=1}^{2}\int_{z_l}^{t_l} f(u-y,\eta)du} f^{(w)}(z_2 - y, \eta)\mu(\mathrm{d}y, \mathrm{d}\eta) \right) \\
&= \left\langle \mathrm{e}^{-\int_{z_1}^{t_1} Q_0(u,\xi)du - \int_{z_2}^{t_2} Q_0(u,\xi)du} \right\rangle \\
&\quad \times \left(\sum_{k=1}^{N} w_k^2 \int_{(-\infty,\min(z_1,z_2)]\times S} \mathrm{e}^{-\frac{1}{\tau}\int_{z_1}^{t_1} g_k(u-y,\eta)du - \frac{1}{\tau}\int_{z_2}^{t_2} g_k(u-y,\eta)du} g_k(z_1 - y, \eta) g_k(z_2 - y, \eta)\mu(\mathrm{d}y, \mathrm{d}\eta) \right. \\
&\quad + \sum_{k,l=1}^{N} w_k w_l \int_{(-\infty,z_1]\times S} \mathrm{e}^{-\frac{1}{\tau}\int_{z_1}^{t_1} g_k(u-y,\eta)du - \frac{1}{\tau}\int_{z_2}^{t_2} g_k(u-y,\eta)du} g_k(z_1 - y, \eta)\mu(\mathrm{d}y, \mathrm{d}\eta) \\
&\quad \left. \times \int_{(-\infty,z_2]\times S} \mathrm{e}^{-\frac{1}{\tau}\int_{z_1}^{t_1} g_l(u-y,\eta)du - \frac{1}{\tau}\int_{z_2}^{t_2} g_l(u-y,\eta)du} g_l(z_2 - y, \eta)\mu(\mathrm{d}y, \mathrm{d}\eta) \right),
\end{aligned} \tag{3.2}$$

which recovers Appendix A page 11 of Brigham and Destexhe (2015a).

Figure 2 presents numerical simulations of first moment and standard deviation in the unit-less single source model (2.13) of Figure 1, together with the mean obtained by Monte Carlo simulations, and is consistent with Figure 1 in Brigham and Destexhe (2015b).

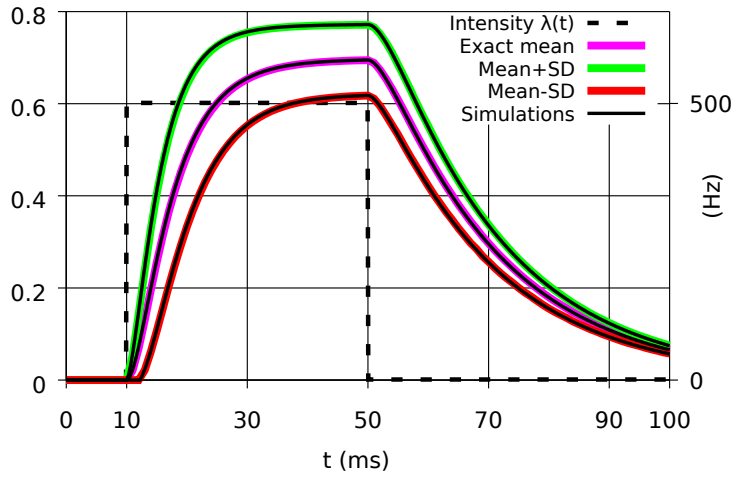

Figure 2: Mean and standard deviation of $Y_1(t,\xi)$ with $\lambda(t) = \lambda \mathbf{1}_{[t_a,t_b]}(t)$.

The next Figure 3 presents estimates of the correlations $\mathrm{Cor}(Y_1(t_1,\xi), Y_1(t_1+t,\xi))$ and of the second joint moments $\langle Y_1(t_1,\xi)Y_1(t_1+t,\xi)\rangle$, with $t_1 := 25\text{ms}$ and $t \in [0, 20\text{ms}]$.

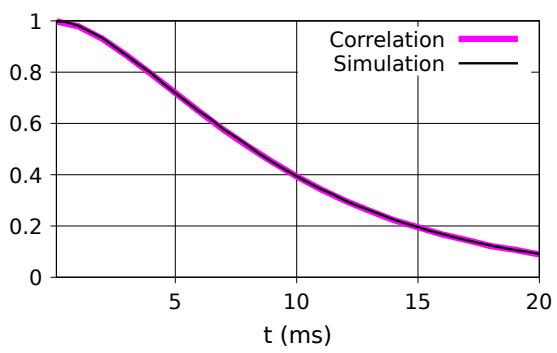

(a) Correlations.

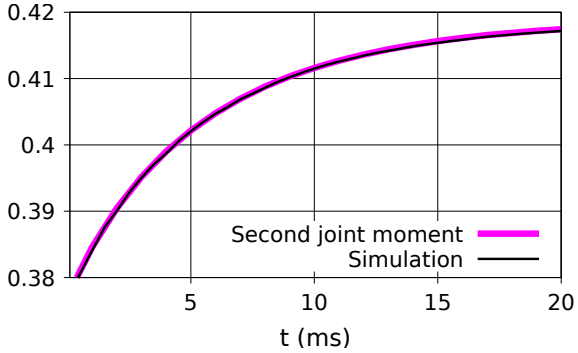

(b) Second joint moments.

Figure 3: Correlation and second joint moments of $Y_1(t_1,\xi)$ and $Y_1(t_1+t,\xi)$.

The following exact analytical formulas for third and fourth moments follow from the application of Proposition 2.2 with $n = 3, 4$.

Third joint moment

When $n = 3$ there are 5 partitions of $\{1, 2, 3\}$, which can be listed as

$\pi_1 =$ '123',

$\pi_1|\pi_2 =$ '12|3'; '1|23'; '13|2',

$\pi_1|\pi_2|\pi_3 =$ '1|2|3',

hence by (2.4) the third joint moment $\langle Y_N(t_1,\xi)Y_N(t_2,\xi)Y_N(t_3,\xi)\rangle$ can be computed from

$$
\begin{aligned}
m_{3,N}(z_1,z_2,z_3;t_1,t_2,t_3) &= \left\langle \mathrm{e}^{-\sum_{l=1}^3 \int_{z_l}^{t_l} Q_0(u,\xi)du} \prod_{l=1}^3 \int_{(-\infty,z_l]\times S} f^{(w)}(z_l-u,\theta)\xi(du,d\theta) \right\rangle \\
&= \left\langle \mathrm{e}^{-\sum_{l=1}^3 \int_{z_l}^{t_l} Q_0(u,\xi)du} \right\rangle \sum_{\pi\in\Pi[3]} \prod_{j=1}^{|\pi|} \int_{(-\infty,\hat{z}_{\pi_j}]\times S} \mathrm{e}^{-\frac{1}{\tau}\sum_{l=1}^3 \int_{z_l}^{t_l} f(u-y,\eta)du} \prod_{i\in\pi_j} f^{(w)}(z_i-y,\eta)\mu(\mathrm{d}y,\mathrm{d}\eta) \\
&= \left\langle \mathrm{e}^{-\sum_{l=1}^3 \int_{z_l}^{t_l} Q_0(u,\xi)du} \right\rangle \Bigg(\int_{(-\infty,\min(z_1,z_2,z_3)]\times S} \mathrm{e}^{-\frac{1}{\tau}\sum_{l=1}^3 \int_{z_l}^{t_l} f(u-y,\eta)du} \prod_{i=1}^3 f^{(w)}(z_i-y,\eta)\mu(\mathrm{d}y,\mathrm{d}\eta) \\
&\quad + \sum_{\pi_1\cup\pi_2=\{1,2,3\}} \prod_{j=1}^2 \int\int_{(-\infty,\hat{z}_{\pi_j}]\times S} \mathrm{e}^{-\frac{1}{\tau}\sum_{l=1}^3 \int_{z_l}^{t_l} f(u-y,\eta)du} \prod_{i\in\pi_j} f^{(w)}(z_i-y,\eta)\mu(\mathrm{d}y,\mathrm{d}\eta) \\
&\quad + \prod_{j=1}^3 \int_{(-\infty,z_j]\times S} \mathrm{e}^{-\frac{1}{\tau}\sum_{l=1}^3 \int_{z_l}^{t_l} f(u-y,\eta)du} f^{(w)}(z_j-y,\eta)\mu(\mathrm{d}y,\mathrm{d}\eta) \Bigg) \\
&= \left\langle \mathrm{e}^{-\sum_{l=1}^3 \int_{z_l}^{t_l} Q_0(u,\xi)du} \right\rangle \Bigg(\int_{(-\infty,\min(z_1,z_2,z_3)]\times S} \mathrm{e}^{-\frac{1}{\tau}\sum_{l=1}^3 \int_{z_l}^{t_l} f(u-y,\eta)du} \prod_{i=1}^3 f^{(w)}(z_i-y,\eta)\mu(\mathrm{d}y,\mathrm{d}\eta) \\
&\quad + \int_{(-\infty,\min(z_1,z_2)]\times S} \mathrm{e}^{-\frac{1}{\tau}\sum_{l=1}^3 \int_{z_l}^{t_l} f(u-y,\eta)du} f^{(w)}(z_1-y,\eta)f^{(w)}(z_2-y,\eta)\mu(\mathrm{d}y,\mathrm{d}\eta) \\
&\qquad \times \int_{(-\infty,z_3]\times S} \mathrm{e}^{-\frac{1}{\tau}\sum_{l=1}^3 \int_{z_l}^{t_l} f(u-y,\eta)du} f^{(w)}(z_3-y,\eta)\mu(\mathrm{d}y,\mathrm{d}\eta) \\
&\quad + \int_{(-\infty,\min(z_2,z_3)]\times S} \mathrm{e}^{-\frac{1}{\tau}\sum_{l=1}^3 \int_{z_l}^{t_l} f(u-y,\eta)du} f^{(w)}(z_2-y,\eta)f^{(w)}(z_3-y,\eta)\mu(\mathrm{d}y,\mathrm{d}\eta) \\
&\qquad \times \int_{(-\infty,z_1]\times S} \mathrm{e}^{-\frac{1}{\tau}\sum_{l=1}^3 \int_{z_l}^{t_l} f(u-y,\eta)du} f^{(w)}(z_1-y,\eta)\mu(\mathrm{d}y,\mathrm{d}\eta) \\
&\quad + \int_{(-\infty,\min(z_1,z_3)]\times S} \mathrm{e}^{-\frac{1}{\tau}\sum_{l=1}^3 \int_{z_l}^{t_l} f(u-y,\eta)du} f^{(w)}(z_1-y,\eta)f^{(w)}(z_3-y,\eta)\mu(\mathrm{d}y,\mathrm{d}\eta) \\
&\qquad \times \int_{(-\infty,z_2]\times S} \mathrm{e}^{-\frac{1}{\tau}\sum_{l=1}^3 \int_{z_l}^{t_l} f(u-y,\eta)du} f^{(w)}(z_2-y,\eta)\mu(\mathrm{d}y,\mathrm{d}\eta)
\end{aligned}
$$

$$+\prod_{j=1}^{3}\int_{(-\infty,z_j]\times S} \mathrm{e}^{-\frac{1}{\tau}\sum_{l=1}^{3}\int_{z_l}^{t_l} f(u-y,\eta)du} f^{(w)}(z_j-y,\eta)\mu(\mathrm{d}y,\mathrm{d}\eta)\Big).$$

Third moment

In the case of the third moment $\langle (Y_N(t,\xi))^3\rangle$, the function $m_{3,N}(z_1,z_2,z_3;t,t,t)$ in (2.6) can be evaluated by (2.8), i.e. by symmetrizing in (z_1,z_2,z_3) the simpler expression

$$\Big\langle \mathrm{e}^{-\sum_{l=1}^{3}\int_{z_l}^{t} Q_0(u,\xi)du}\Big\rangle \Big(\int_{(-\infty,\min(z_1,z_2,z_3)]\times S} \mathrm{e}^{-\frac{1}{\tau}\sum_{l=1}^{3}\int_{z_l}^{t} f(u-y,\eta)du} \prod_{i=1}^{3} f^{(w)}(z_i-y,\eta)\mu(\mathrm{d}y,\mathrm{d}\eta)$$
$$+3\int_{(-\infty,\min(z_1,z_2)]\times S} \mathrm{e}^{-\frac{1}{\tau}\sum_{l=1}^{3}\int_{z_l}^{t} f(u-y,\eta)du} f^{(w)}(z_1-y,\eta)f^{(w)}(z_2-y,\eta)\mu(\mathrm{d}y,\mathrm{d}\eta)$$
$$\times\int_{(-\infty,z_3]\times S} \mathrm{e}^{-\frac{1}{\tau}\sum_{l=1}^{3}\int_{z_l}^{t} f(u-y,\eta)du} f^{(w)}(z_3-y,\eta)\mu(\mathrm{d}y,\mathrm{d}\eta)$$
$$+\prod_{j=1}^{3}\int_{(-\infty,z_j]\times S} \mathrm{e}^{-\frac{1}{\tau}\sum_{l=1}^{3}\int_{z_l}^{t_l} f(u-y,\eta)du} f^{(w)}(z_j-y,\eta)\mu(\mathrm{d}y,\mathrm{d}\eta)\Big). \tag{3.3}$$

Fourth moment

For $n=4$ there are 15 partitions of $\{1,2,3,4\}$, which can be listed as

$\pi_1 =$ '1234',

$\pi_1|\pi_2 =$ '12|34'; '13|24'; '14|23'; '1|234'; '2|134'; '3|124'; '4|123',

$\pi_1|\pi_2|\pi_3 =$ '1|2|34'; '1|3|24'; '2|3|14'; '2|4|12'; '1|4|23'; '3|4|12',

$\pi_1|\pi_2|\pi_3|\pi_4 =$ '1|2|3|4'.

Hence, in the case of the fourth moment $\langle (Y_N(t,\xi))^4\rangle$ the function $m_{4,N}(z_1,z_2,z_3,z_4;t,t,t,t)$ can be evaluated by the symmetrization (2.8) of (2.6) in (z_1,z_2,z_3,z_4), as

$$m_{4,N}(z_1,z_2,z_3,z_4;t,t,t,t) = \Big\langle \mathrm{e}^{-\sum_{l=1}^{4}\int_{z_l}^{t} Q_0(u,\xi)du} \prod_{l=1}^{4}\int_{(-\infty,z_l]\times S} f^{(w)}(z_l-u,\theta)\xi(du,d\theta)\Big\rangle$$
$$= \Big\langle \mathrm{e}^{-\sum_{l=1}^{4}\int_{z_l}^{t} Q_0(u,\xi)du}\Big\rangle \Big(\int_{(-\infty,\min(z_1,z_2,z_3,z_4)]\times S} \mathrm{e}^{-\frac{1}{\tau}\sum_{l=1}^{4}\int_{z_l}^{t} f(u-y,\eta)du} \prod_{i=1}^{4} f^{(w)}(z_i-y,\eta)\mu(\mathrm{d}y,\mathrm{d}\eta)$$
$$+3\int\int_{(-\infty,\min(z_1,z_3)]\times S} \mathrm{e}^{-\frac{1}{\tau}\sum_{l=1}^{4}\int_{z_l}^{t} f(u-y,\eta)du} f^{(w)}(z_1-y,\eta)f^{(w)}(z_2-y,\eta)\mu(\mathrm{d}y,\mathrm{d}\eta)$$
$$\times\int\int_{(-\infty,\min(z_3,z_4)]\times S} \mathrm{e}^{-\frac{1}{\tau}\sum_{l=1}^{4}\int_{z_l}^{t_l} f(u-y,\eta)du} f^{(w)}(z_3-y,\eta)f^{(w)}(z_4-y,\eta)\mu(\mathrm{d}y,\mathrm{d}\eta)$$

$$
\begin{aligned}
&+4\int\int_{(-\infty,z_1]\times S} \mathrm{e}^{-\frac{1}{\tau}\sum_{l=1}^4\int_{z_l}^{t_l} f(u-y,\eta)du} f^{(w)}(z_1-y,\eta)\mu(\mathrm{d}y,\mathrm{d}\eta)\\
&\quad\times\int\int_{(-\infty,\min(z_2,z_3,z_4)]\times S} \mathrm{e}^{-\frac{1}{\tau}\sum_{l=1}^4\int_{z_l}^{t_l} f(u-y,\eta)du} f^{(w)}(z_2-y,\eta)f^{(w)}(z_3-y,\eta)f^{(w)}(z_4-y,\eta)\mu(\mathrm{d}y,\mathrm{d}\eta)\\
&+6\int\int_{(-\infty,z_1]\times S} \mathrm{e}^{-\frac{1}{\tau}\sum_{l=1}^4\int_{z_l}^{t_l} f(u-y,\eta)du} f^{(w)}(z_1-y,\eta)\mu(\mathrm{d}y,\mathrm{d}\eta)\\
&\quad\times\int\int_{(-\infty,z_2]\times S} \mathrm{e}^{-\frac{1}{\tau}\sum_{l=1}^4\int_{z_l}^{t_l} f(u-y,\eta)du} f^{(w)}(z_2-y,\eta)\mu(\mathrm{d}y,\mathrm{d}\eta)\\
&\quad\times\int\int_{(-\infty,\min(z_3,z_4)]\times S} \mathrm{e}^{-\frac{1}{\tau}\sum_{l=1}^4\int_{z_l}^{t_l} f(u-y,\eta)du} (z_3-y,\eta)f^{(w)}(z_4-y,\eta)\mu(\mathrm{d}y,\mathrm{d}\eta)\\
&+\prod_{j=1}^4\int_{(-\infty,z_j]\times S} \mathrm{e}^{-\frac{1}{\tau}\sum_{l=1}^4\int_{z_l}^{t_l} f(u-y,\eta)du} f^{(w)}(z_j-y,\eta)\mu(\mathrm{d}y,\mathrm{d}\eta)\Big). \qquad (3.4)
\end{aligned}
$$

When $f(v,\theta)=g_1(v,\theta):=h\mathrm{e}^{-v/\tau_s}\mathbf{1}_{[0,\infty)}(v)$, the integral $\int_z^t f(u-y,\theta)du$ in (2.7) can be computed for $y<t$ as

$$
\begin{aligned}
\int_z^t f(u-y,\theta)du &= \int_z^t g_1(u-y,\theta)du\\
&= \int_{\max(y,z)}^t g_1(u-y,\theta)du\\
&= h\mathrm{e}^{y/\tau_s}\int_{\max(y,z)}^t \mathrm{e}^{-u/\tau_s}du\\
&= h\tau_s\big(\mathrm{e}^{-(z-y)^+/\tau_s}-\mathrm{e}^{(y-t)/\tau_s}\big), \qquad y,z\le t. \qquad (3.5)
\end{aligned}
$$

The next Figure 4 presents numerical estimates of the exact third and fourth moment expressions (3.3)-(3.4) for the membrane potential $Y_1(t,\xi)$ in the unit-less single source model (2.13) of Figures 1-2.

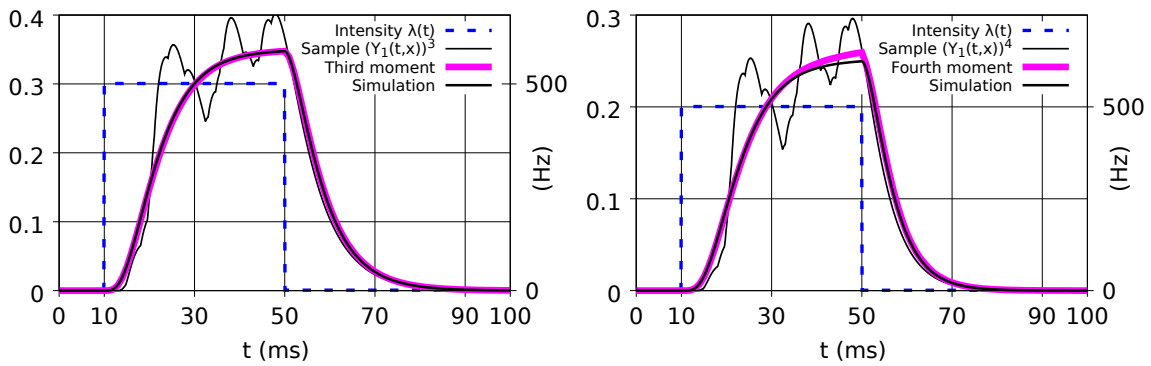

(a) Third moments of $Y_1(t,\xi)$. (b) Fourth moments of $Y_1(t,\xi)$.

Figure 4: Third and fourth moments of $Y_1(t,\xi)$.

4 Cumulants and Gram-Charlier expansions

In this section we review the method of approximation of probability density functions by Gram-Charlier expansions. Existence of the probability density of $Y_1(t,\xi)$ given that $\xi([0,t]\times S) \geq 1$ can be proved when $f^{(w)}(z,\theta) = w_1 g_1(z,\theta)$ is a decreasing function of $z \in \mathbb{R}$, using e.g. the results of Privault and Torrisi (2011), see Lemma 7.2 and Propositions 4.1-6.1 therein. Gram-Charlier expansions also make sense as smoothed density approximations in the case of discrete distributions which do not admit a probability density.

4.1 Joint cumulants

In this section, we present the computation of the first four cumulants of $Y_N(t,\xi)$ in the multiple source model, based on the results of Section 3. We start with the first two cumulants, in which case our results coincide with Brigham and Destexhe (2015a;b). The joint cumulants $\langle\langle Y_N(t_1,\xi)\cdots Y_N(t_n,\xi)\rangle\rangle$ can be recovered from the joint cumulant-moment relationship

$$\langle\langle X_1\cdots X_n\rangle\rangle = \sum_{\pi\in\Pi[n]} (|\pi|-1)!(-1)^{|\pi|-1}\prod_{j=1}^{|\pi|}\left\langle\prod_{i\in\pi_j} X_i\right\rangle, \tag{4.1}$$

which can be obtained by Möbius inversion of moment-cumulant relation

$$\langle X_1\cdots X_n\rangle = \sum_{\pi\in\Pi[n]}\prod_{j=1}^{|\pi|}\left\langle\left\langle\prod_{i\in\pi_j} X_i\right\rangle\right\rangle, \tag{4.2}$$

see Theorem 1 in Lukacs (1955) or Relation (2.9) in McCullagh (1987). In particular:

i) The first cumulant $\langle\langle Y_N(t_1,\xi)\rangle\rangle = \langle Y_N(t_1,\xi)\rangle$ is the mean of $Y_N(t_1,\xi)$.

ii) The second joint cumulant

$$\begin{aligned}\langle\langle Y_N(t_1,\xi)Y_N(t_2,\xi)\rangle\rangle &= \langle Y_N(t_1,\xi)Y_N(t_2,\xi)\rangle - \langle Y_N(t_1,\xi)\rangle\langle Y_N(t_2,\xi)\rangle \\ &= \langle (Y_N(t_1,\xi)-\langle Y_N(t_1,\xi)\rangle)(Y_N(t_2,\xi)-\langle Y_N(t_2,\xi)\rangle)\rangle \\ &= \mathrm{Cov}(Y_N(t_1,\xi),Y_N(t_2,\xi))\end{aligned}$$

coincides with the covariance, or second joint central moment, of $Y_N(t_1,\xi)$, $Y_N(t_2,\xi)$.

iii) The third joint cumulant of $Y_N(t_1,\xi), Y_N(t_2,\xi), Y_N(t_3,\xi)$, given by

$$\begin{aligned}&\langle\langle Y_N(t_1,\xi)Y_N(t_2,\xi)Y_N(t_3,\xi)\rangle\rangle \qquad (4.3)\\ &= \sum_{\pi_1=\{1,2,3\}}\left\langle\prod_{i\in\pi_1}Y_N(t_i,\xi)\right\rangle - \sum_{\pi_1\cup\pi_2=\{1,2,3\}}\left\langle\prod_{i\in\pi_1}Y_N(t_i,\xi)\right\rangle\left\langle\prod_{i\in\pi_2}Y_N(t_i,\xi)\right\rangle \\ &\quad +2\sum_{\pi_1\cup\pi_2\cup\pi_3=\{1,2,3\}}\left\langle\prod_{i\in\pi_1}Y_N(t_i,\xi)\right\rangle\left\langle\prod_{i\in\pi_2}Y_N(t_i,\xi)\right\rangle\left\langle\prod_{i\in\pi_3}Y_N(t_i,\xi)\right\rangle \\ &= \langle Y_N(t_1,\xi)Y_N(t_2,\xi)Y_N(t_3,\xi)\rangle - \langle Y_N(t_1,\xi)Y_N(t_2,\xi)\rangle\langle Y_N(t_3,\xi)\rangle \\ &\quad -\langle Y_N(t_1,\xi)Y_N(t_3,\xi)\rangle\langle Y_N(t_2,\xi)\rangle - \langle Y_N(t_2,\xi)Y_N(t_3,\xi)\rangle\langle Y_N(t_1,\xi)\rangle \\ &\quad +2\langle Y_N(t_1,\xi)\rangle\langle Y_N(t_2,\xi)\rangle\langle Y_N(t_3,\xi)\rangle \\ &= \big\langle\big(Y_N(t_1,\xi)-\langle Y_N(t_1,\xi)\rangle\big)\big(Y_N(t_2,\xi)-\langle Y_N(t_2,\xi)\rangle\big)\big(Y_N(t_3,\xi)-\langle Y_N(t_3,\xi)\rangle\big)\big\rangle,\end{aligned}$$

coincides with the third joint central moment of $Y_N(t_1,\xi), Y_N(t_2,\xi), Y_N(t_3,\xi)$, while

$$\frac{\langle\langle (Y_N(t,\xi))^3\rangle\rangle}{(\langle\langle (Y_N(t,\xi))^2\rangle\rangle)^{3/2}} = \frac{\langle (Y_N(t,\xi)-\langle Y_N(t,\xi)\rangle)^3\rangle}{(\langle (Y_N(t,\xi)-\langle Y_N(t,\xi)\rangle)^2\rangle)^{3/2}}$$

is the skewness of $Y_N(t,\xi)$.

iv) The fourth joint cumulant of $Y_N(t_1,\xi), Y_N(t_2,\xi), Y_N(t_3,\xi), Y_N(t_4,\xi)$ is given by

$$\begin{aligned}\langle\langle Y_N(t_1,\xi)Y_N(t_2,\xi)Y_N(t_3,\xi)Y_N(t_4,\xi)\rangle\rangle &= \left\langle\prod_{i=1}^4\big(Y_N(t_i,\xi)-\langle Y_N(t_i,\xi)\rangle\big)\right\rangle \qquad (4.4)\\ &\quad -\big\langle(Y_N(t_1,\xi)-\langle Y_N(t_1,\xi)\rangle)(Y_N(t_2,\xi)-\langle Y_N(t_2,\xi)\rangle)\big\rangle \\ &\quad \times\big\langle(Y_N(t_3,\xi)-\langle Y_N(t_3,\xi)\rangle)(Y_N(t_4,\xi)-\langle Y_N(t_4,\xi)\rangle)\big\rangle\end{aligned}$$

$$
\begin{aligned}
&-\big\langle (Y_N(t_1,\xi)-\langle Y_N(t_1,\xi)\rangle)(Y_N(t_3,\xi)-\langle Y_N(t_3,\xi)\rangle)\big\rangle\\
&\quad\times\big\langle (Y_N(t_2,\xi)-\langle Y_N(t_2,\xi)\rangle)(Y_N(t_4,\xi)-\langle Y_N(t_4,\xi)\rangle)\big\rangle\\
&-\big\langle (Y_N(t_1,\xi)-\langle Y_N(t_1,\xi)\rangle)(Y_N(t_4,\xi)-\langle Y_N(t_4,\xi)\rangle)\big\rangle\\
&\quad\times\big\langle (Y_N(t_2,\xi)-\langle Y_N(t_2,\xi)\rangle)(Y_N(t_3,\xi)-\langle Y_N(t_3,\xi)\rangle)\big\rangle,
\end{aligned}
$$

and the excess kurtosis of $Y_N(t,\xi)$ is defined as

$$
\frac{\langle\langle (Y_N(t,\xi))^4\rangle\rangle}{(\langle\langle (Y_N(t,\xi))^2\rangle\rangle)^2}=\frac{\big\langle (Y_N(t,\xi)-\langle Y_N(t,\xi)\rangle)^4\big\rangle}{(\langle\langle (Y_N(t,\xi)-\langle Y_N(t,\xi)\rangle)^2\rangle\rangle)^2}-3.
$$

4.2 Gram-Charlier expansions

Let now

$$
\varphi(x):=\frac{1}{\sqrt{2\pi}}\mathrm{e}^{-x^2/2},\qquad x\in\mathbb{R},
$$

denote the standard normal density function, and let

$$
H_n(x):=\frac{(-1)^n}{\varphi(x)}\frac{\partial^n\varphi}{\partial x^n}(x),\qquad x\in\mathbb{R},
$$

denote the Hermite polynomial of degree n, with $H_0(x)=1$, $H_1(x)=x$, $H_3(x)=x^3-3x$, $H_4(x)=x^4-6x^2+3$, $H_6(x)=x^6-15x^4+45x^2-15$. Next, we summarize the Gram-Charlier expansion method to obtain series expansion of a probability density function, see § 17.6 of Cramér (1946).

Proposition 4.1 *The Gram-Charlier expansion of the continuous probability density function $\phi_X(x)$ of a random variable X is given by*

$$
\phi_X(x)=\frac{1}{\sqrt{\kappa_2}}\varphi\left(\frac{x-\kappa_1}{\sqrt{\kappa_2}}\right)+\frac{1}{\sqrt{\kappa_2}}\sum_{n=3}^{\infty}c_nH_n\left(\frac{x-\kappa_1}{\sqrt{\kappa_2}}\right)\varphi\left(\frac{x-\kappa_1}{\sqrt{\kappa_2}}\right),\tag{4.5}
$$

where the sequence $(c_n)_{n\geq 3}$ is given from the cumulants $(\kappa_n)_{n\geq 1}$ of X as

$$
c_n=\frac{1}{\kappa_2^{n/2}}\sum_{m=1}^{[n/3]}\sum_{\substack{l_1+\cdots+l_m=n\\ l_1,\ldots,l_m\geq 3}}\frac{\kappa_{l_1}\cdots\kappa_{l_m}}{m!l_1!\cdots l_m!},\qquad n\geq 3.
$$

In particular, the coefficients c_3 and c_4 can be expressed from the skweness $\kappa_3/\kappa_2^{3/2}$ and the excess kurtosis κ_4/κ_2^2 as

$$
c_3=\frac{\kappa_3}{3!\kappa_2^{3/2}}\quad\text{and}\quad c_4=\frac{\kappa_4}{4!\kappa_2^2},
$$

with

$$c_5 = \frac{\kappa_5^2}{5!\kappa_5}, \quad \text{and} \quad c_6 = \frac{\kappa_6}{6!\kappa_2^3} + \frac{\kappa_3^2}{2(3!)^2\kappa_2^3}.$$

In the sequel we will only use c_3, c_4 and $c_6 = \kappa_3^2/(2(3!)^2\kappa_2^3)$ due to the unavailability of κ_5 and κ_6 in our approach. The first-order expansion

$$\phi_X^{(1)}(x) = \frac{1}{\sqrt{\kappa_2}}\varphi\left(\frac{x-\kappa_1}{\sqrt{\kappa_2}}\right) \tag{4.6}$$

corresponds to the diffusion approximation (2.10), and the third and fourth-order expansions are given by

$$\phi_X^{(3)}(x) = \frac{1}{\sqrt{\kappa_2}}\varphi\left(\frac{x-\kappa_1}{\sqrt{\kappa_2}}\right)\left(1 + c_3 H_3\left(\frac{x-\kappa_1}{\sqrt{\kappa_2}}\right)\right) \tag{4.7}$$

and

$$\phi_X^{(4)}(x) = \frac{1}{\sqrt{\kappa_2}}\varphi\left(\frac{x-\kappa_1}{\sqrt{\kappa_2}}\right)\left(1 + c_3 H_3\left(\frac{x-\kappa_1}{\sqrt{\kappa_2}}\right) + c_4 H_4\left(\frac{x-\kappa_1}{\sqrt{\kappa_2}}\right) + c_6 H_6\left(\frac{x-\kappa_1}{\sqrt{\kappa_2}}\right)\right). \tag{4.8}$$

4.3 Single source model

Figure 5 presents time-dependent numerical estimates of the third and fourth cumulant formulas (4.3)-(4.4) for the membrane potential $Y_1(t,\xi)$, based on the exact moment expressions (3.1)-(3.4) in the unit-less single source model (2.13) of Figures 1 and 2.

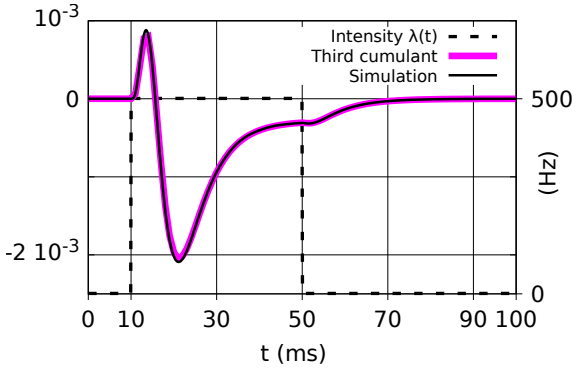

(a) Third cumulants of $Y_1(t,\xi)$.

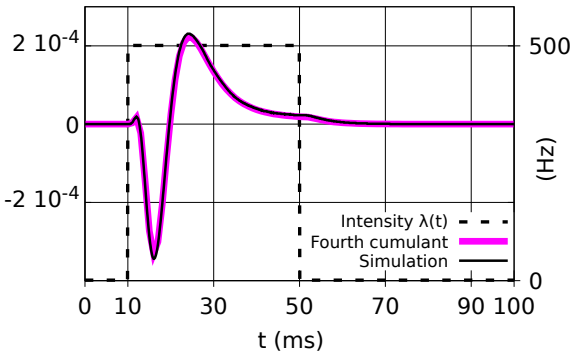

(b) Fourth cumulants of $Y_1(t,\xi)$.

Figure 5: Third and fourth cumulants of $Y_1(t,\xi)$.

The next Figures 6 and 7 present estimates of the third joint cumulants and third joint moments of $\big(Y_1(t_1,\xi), Y_1(t_1,\xi), Y_1(t_1+t,\xi)\big)$ and $\big(Y_1(t_1,\xi), Y_1(t_2,\xi), Y_1(t_1+t,\xi)\big)$ respectively, with $t_1 := 25\text{ms}$, $t_2 := 35\text{ms}$, and $t \in [0, 20\text{ms}]$.

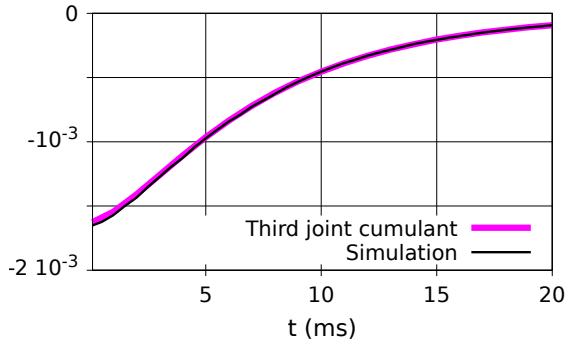

(a) Third joint cumulants.

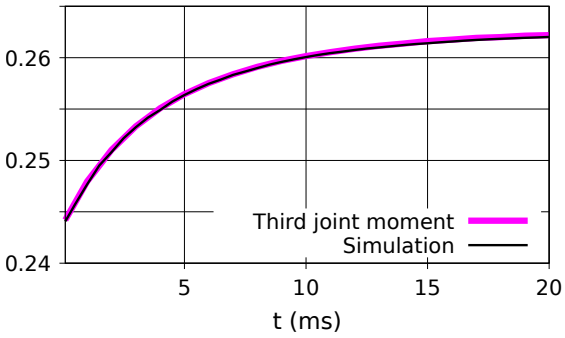

(b) Third joint moments.

Figure 6: Third joint cumulants and moments of $\big(Y_1(t_1,\xi), Y_1(t_1,\xi), Y_1(t_1+t,\xi)\big)$.

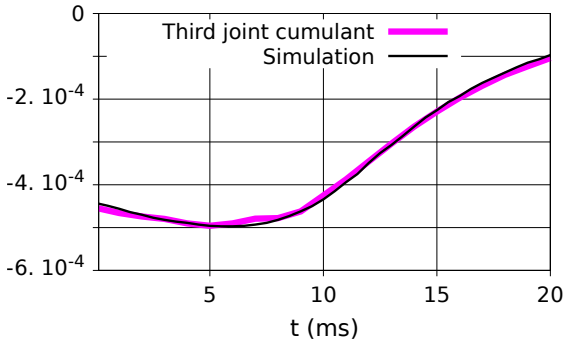

(a) Third joint cumulants.

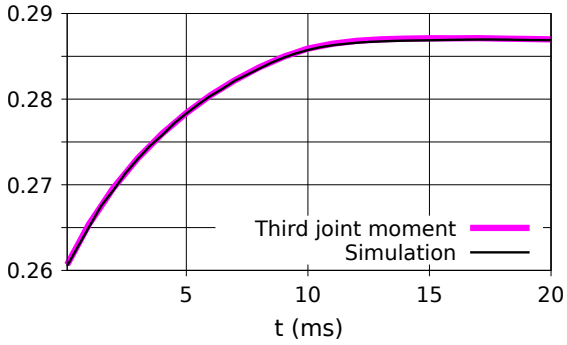

(b) Third joint moments.

Figure 7: Third joint cumulants and moments of $\big(Y_1(t_1,\xi), Y_1(t_2,\xi), Y_1(t_1+t,\xi)\big)$.

Figure 8 presents numerical estimates of skewness $\langle\langle X^3\rangle\rangle/(\langle\langle X^2\rangle\rangle)^{3/2}$ and excess kurtosis $\langle\langle X^4\rangle\rangle/(\langle\langle X^2\rangle\rangle)^2$ obtained from the exact moment expressions (3.2)-(3.4) in the single source model (2.13). Negative skewness and positive excess kurtosis are observed starting after $t = 20\text{ms}$.

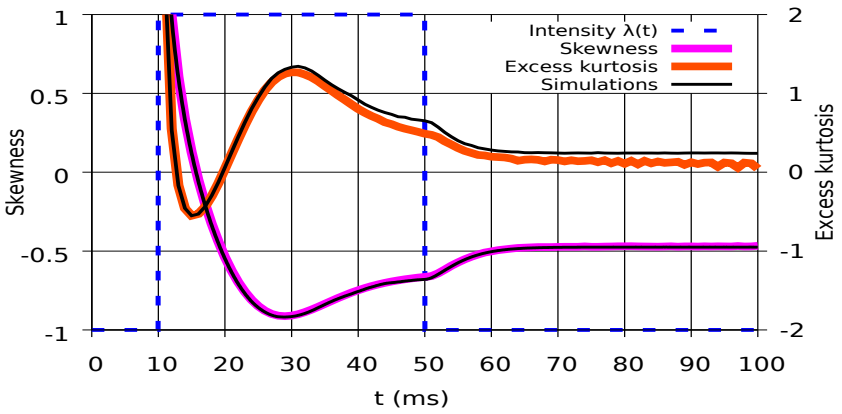

Figure 8: Skewness and excess kurtosis of $Y_1(t, \xi)$.

The next Figure 9 presents second, third and fourth-order Gram-Charlier expansions (4.5) based on the exact moment expressions (3.1)-(3.4) computed at different times, for the probability density function of the membrane potential $Y_1(t, \xi)$ in the single source model (2.13) of Figures 1 and 2. The purple areas correspond to probability density estimates obtained by Monte Carlo simulations of the numerical solution of (2.1). The second-order expansions correspond to the Gaussian diffusion approximation (2.10) obtained by matching (2.11)-(2.12) to the first and second-order moments (3.1)-(3.2).

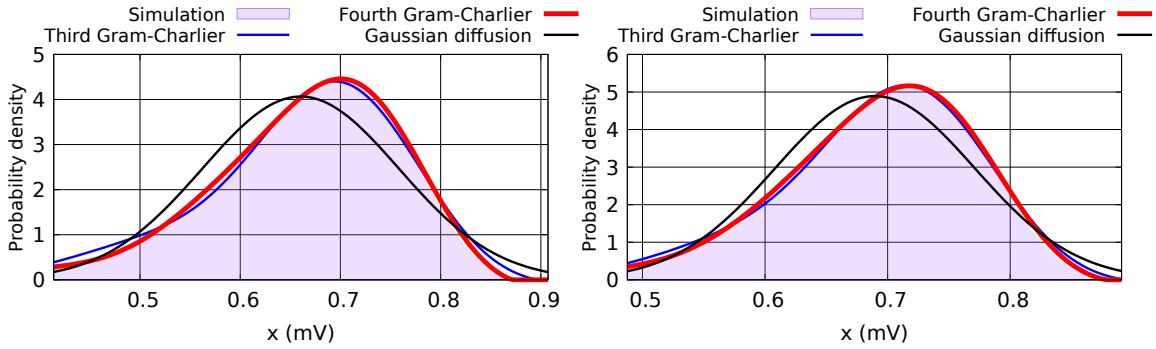

(a) t=30 ms. (b) t=40 ms.

Figure 9: Gram-Charlier density expansions *vs* Monte Carlo density estimation.

The actual probability density estimates obtained by simulation show significant differences from their Gaussian diffusion approximations when skewness and kurtosis take their largest absolute values. In addition, in Figure 9 the fourth-order Gram-Charlier expansions appear to give the best fit to the actual probability densities,

which have negative skewness and positive excess kurtosis, see Figure 8, and the impact of the fourth cumulant remains minimal.

Figure 10 presents time-dependent fourth-order Gram-Charlier expansions (4.5), based on the exact moment formulas (3.2)-(3.4) at different times, for the probability density function of $Y_1(t,\xi)$ in the single source model (2.13) of Figure 1 and 2.

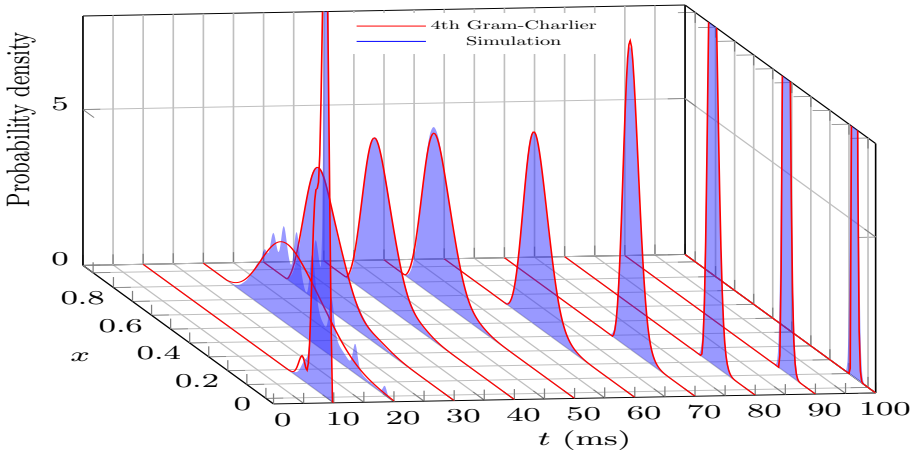

Figure 10: Fourth-order Gram-Charlier expansions vs simulated densities.

As can be checked from Figure 10, the fourth-order Gram-Charlier expansions fit the purple areas obtained by Monte Carlo simulation of the numerical solution of (2.1). Figure 11-a) compares the Gaussian diffusion (blue) approximation to the fourth-order Gram-Charlier expansion (purple) for the probability density function of $Y_1(t,\xi)$ in the unit-less single source model (2.13), while Figure 11-b) represents the relative difference between the Gaussian diffusion and fourth-order approximations.

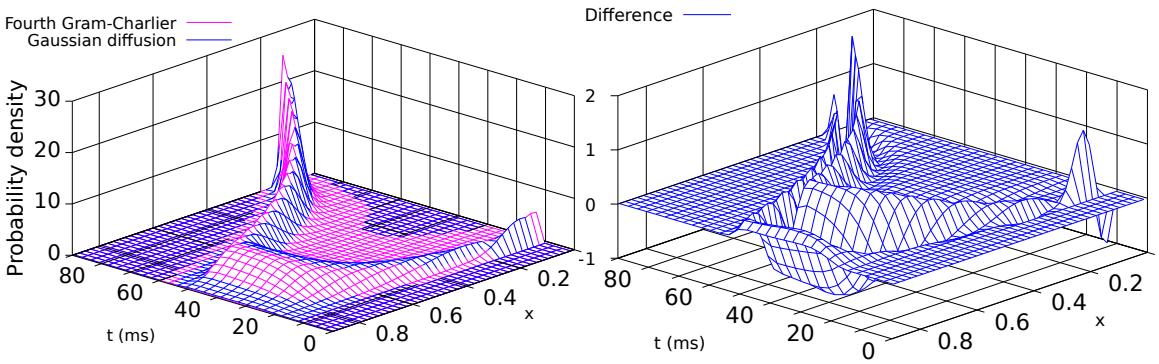

(a) Gaussian diffusion *vs* 4th Edgeworth. (b) Difference between 2nd and 4th Edgeworth.

Figure 11: Fourth-order Gram-Charlier expansion *vs* diffusion approximation.

4.4 Double source model

In this section we consider the Gram-Charlier probability density expansions obtained in a nonstationary double source model, with $N = 2$ and $S = [0, 2]$. In this case, Proposition 5.6 in the appendix reads

$$
\begin{aligned}
&m_{n,2}(z_1, \ldots, z_n; t_1, \ldots, t_n) \\
&= \left\langle \mathrm{e}^{-\frac{1}{\tau}\sum_{l=1}^n \int_{z_l}^{t_l} Q_0(u,\xi)du} \right\rangle \sum_{\pi\in\Pi[n]} \prod_{j=1}^{|\pi|} \int_{(-\infty,\hat{z}_{\pi_j}]\times[0,1]} \prod_{l=1}^n \mathrm{e}^{-\frac{1}{\tau}\int_{z_l}^{t_l} g_1(u-y,\eta)du} \prod_{i\in\pi_j} g_1(z_i - y, \eta)\lambda_1(y)dyd\eta \\
&+ \left\langle \mathrm{e}^{-\frac{1}{\tau}\sum_{l=1}^n \int_{z_l}^{t_l} Q_0(u,\xi)du} \right\rangle \sum_{\pi\in\Pi[n]} \prod_{j=1}^{|\pi|} \int_{(-\infty,\hat{z}_{\pi_j}]\times[1,2]} \prod_{l=1}^n \mathrm{e}^{-\frac{1}{\tau}\int_{z_l}^{t_l} g_2(u-y,\eta)du} \prod_{i\in\pi_j} g_2(z_i - y, \eta)\lambda_2(y)dyd\eta,
\end{aligned}
$$

$(z_1, \ldots, z_n) \in (-\infty, t_1] \times \cdots \times (-\infty, t_n]$, where

$$
\begin{aligned}
\left\langle \mathrm{e}^{-\frac{1}{\tau}\sum_{l=1}^n \int_{z_l}^{t_l} Q_0(u,\xi)du} \right\rangle &= \mathrm{e}^{-\frac{1}{\tau}\sum_{l=1}^n (t-z_l)} \exp\left(\int_{(-\infty,t]\times[0,1]} (\mathrm{e}^{-\frac{1}{\tau}\sum_{l=1}^n \int_{z_l}^{t_l} g_1(u-y,\eta)du} - 1)\lambda_1(y)dyd\eta \right) \\
&\quad \times \exp\left(\int_{(-\infty,t]\times[1,2]} (\mathrm{e}^{-\frac{1}{\tau}\sum_{l=1}^n \int_{z_l}^{t_l} g_2(u-y,\eta)du} - 1)\lambda_2(y)dyd\eta \right),
\end{aligned}
$$

and the third and fourth moments are computed from the exact expressions (3.3)-(3.4). We have

$$
f^{(w)}(z,\theta) = w_1 g_1(z,\theta) + w_2 g_2(z,\theta), \qquad f(z,\theta) = g_1(z,\theta) + g_2(z,\theta),
$$

with

$$
\mu(dx, d\theta) = \lambda_1(x)\mathbf{1}_{[0,1]}(\theta)dxd\theta + \lambda_2(x)\mathbf{1}_{[1,2]}(\theta)dxd\theta, \quad x \in \mathbb{R},\ \theta \in [0,2],
$$

where

$$
g_1(v,\theta) = h_1 \mathrm{e}^{-v/\tau_s}\mathbf{1}_{[0,\infty)}(v)\mathbf{1}_{[0,1]}(\theta), \qquad g_2(v,\theta) = h_2 \frac{v}{\tau_s}\mathrm{e}^{-v/\tau_s}\mathbf{1}_{[0,\infty)}(v)\mathbf{1}_{[1,2]}(\theta),
$$

and

$$
Q_0(t,\xi) = 1 + \int_{(-\infty,t]\times[0,1]} g_1(t-u,\theta)\xi(du,d\theta) + \int_{(-\infty,t]\times[1,2]} g_2(t-u,\theta)\xi(du,d\theta).
$$

Here, the integral $\int_z^t g_1(u-y,\theta)du$ is given for $y < t$ by (3.5), $\theta \in [0,1]$, and we have

$$
\int_z^t g_2(u-y,\theta)du \quad = \quad \int_{\max(y,z)}^t g_2(u-y,\theta)du
$$

$$= \frac{h_2}{\tau_s} e^{y/\tau_s} \int_{\max(y,z)}^{t} u e^{-u/\tau_s} du - \frac{h_2}{\tau_s} y e^{y/\tau_s} \int_{\max(y,z)}^{t} e^{-u/\tau_s} du$$
$$= h_2 e^{-(z-y)^+/\tau_s} (\max(y,z) + \tau_s - y) - h_2 e^{(y-t)/\tau_s} (t + \tau_s - y),$$

$\theta \in [1,2]$. The following numerical examples use the parameters of Brigham and Destexhe (2015a) for excitatory and inhibitory shot noise conductances, i.e. $\tau = 0.02$s, $\tau_s = 0.0025$s, $h_1 = h_e = 2\text{e}{-9}/10\text{e}{-9} = 0.2$, $h_2 = h_i = 15\text{e}{-9}/10\text{e}{-9} = 1.5$, $E_1 = E_e = 0.0V$, $E_2 = Ei = -0.08V$, $E_l = -0.06V$, $w_1 = w_e = (E_e - E_l)/(E_e - E_i) = 0.75$, $w_2 = w_i = (E_i - E_l)/(E_e - E_i) = -0.25$, while $\lambda_2(t) = \lambda_i(t) = 500$Hz, $t \in [0, 100]$, and $\lambda_1(t) = \lambda_e(t)$ is the nonstationary intensity

$$\lambda_e(t) = 200 \times \left(\max\left(0, \left|\sin\left(4\pi \frac{u}{T}\right)\right| - \frac{3}{4}\right)\right) \left(5 - \sin\left(4\pi \frac{u}{T}\right)\right) \left(7 + \sin\left(\frac{2\pi u}{T}\right)\right),$$

$t \in [0, 100]$. The next figures are plotted for the voltage potential

$$V_2(t,\xi) = E_l + (E_e - E_i) Y_2(t,\xi), \tag{4.9}$$

which solves the equation

$$\tau \frac{dV_N}{dt}(t,\xi) = E_l - V_N(t,\xi) + \sum_{k=1}^{N} (E_k - V_N(t,\xi)) Q_k(t,\xi) \tag{4.10}$$

for $N = 2$. Figure 12 presents random simulations of the shot noise processes $Q_1(t,\xi)$ and $Q_2(t,\xi)$.

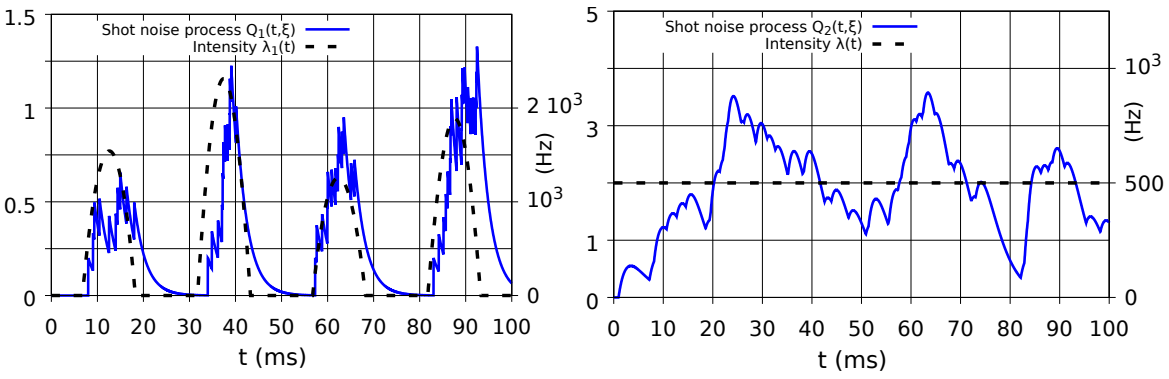

(a) Shot noise process with intensity $\lambda_e(t)$. (b) Shot noise process with intensity $\lambda_i(t)$.

Figure 12: Shot noise processes $Q_1(t,\xi)$ and $Q_2(t,\xi)$.

Figure 13 presents numerical simulations of first moment and standard deviation, together with the mean obtained by Monte Carlo simulation for $V_2(t,\xi) = E_l + (E_e - E_i) Y_2(t,\xi)$, and is consistent with Figure 3 in Brigham and Destexhe (2015a).

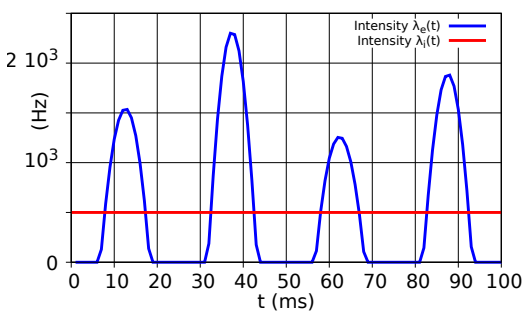

(a) Intensities $\lambda_e(t)$ and $\lambda_i(t)$.

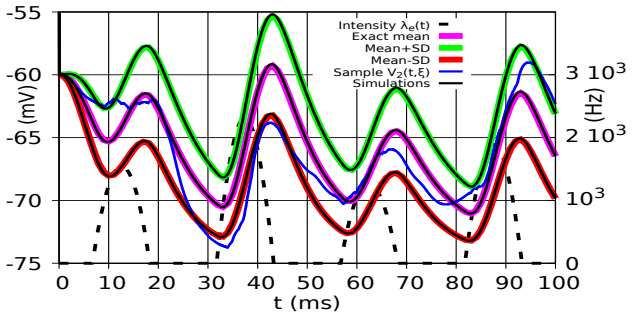

(b) Mean and standard deviation of $V_2(t, \xi)$.

Figure 13: Sample of $V_2(t, \xi)$ with mean, standard deviation and intensities $\lambda_1(t)$, $\lambda_2(t)$.

Figure 14 presents estimates of the correlations $\mathrm{Cor}(V_2(t_1, \xi), V_2(t_1 + t, \xi))$ and of the second joint moments $\langle V_2(t_1, \xi) V_2(t_1 + t, \xi) \rangle$ with $t_1 := 35\text{ms}$ and $t \in [0, 20\text{ms}]$.

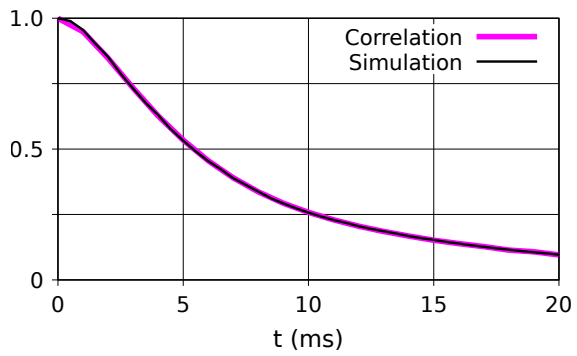

(a) Correlations.

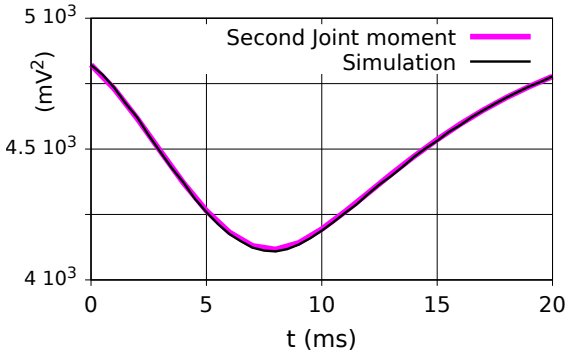

(b) Second joint moments.

Figure 14: Correlations and second joint moments of $V_2(t_1, \xi)$ and $V_2(t_1 + t, \xi)$.

The next Figure 15 presents numerical estimates of the exact third and fourth moment expressions (3.3)-(3.4) for the membrane potential $V_2(t, \xi)$ in the double source model.

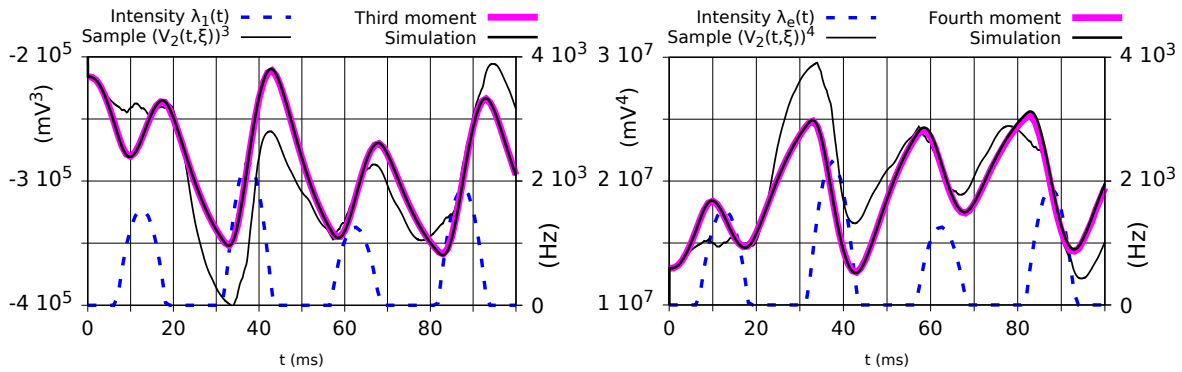

(a) Third moment of $V_2(t,\xi)$. (b) Fourth moment of $V_2(t,\xi)$.

Figure 15: Third and fourth moments of $V_2(t,\xi)$.

Figure 16 presents time-dependent numerical estimates of third and fourth cumulants (4.3)-(4.4) of the membrane potential $V_2(t,\xi)$, based on the exact expressions (3.2)-(3.4) in the double source model (2.2) of Figure 13. The numerical instabilities observed in Figure 16-b) for the Monte Carlo computation of fourth cumulants with one million samples appear to remain even after increasing the number of samples up to 100 million.

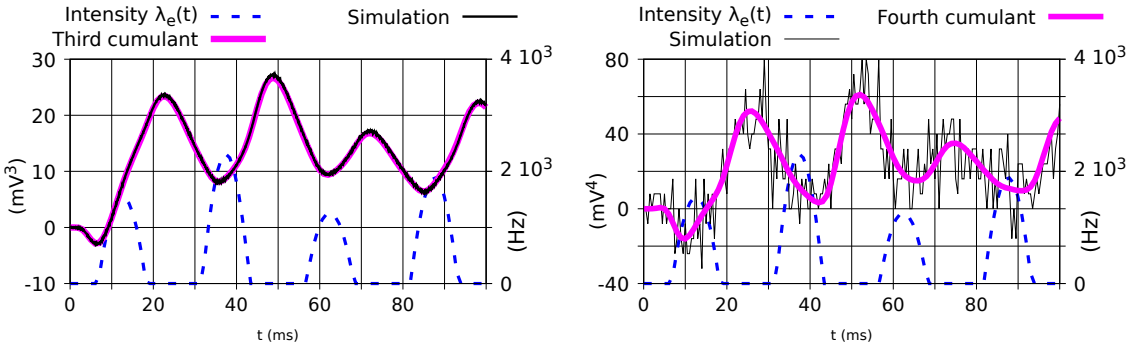

(a) Third cumulant of $V_2(t,\xi)$. (b) Fourth cumulant of $V_2(t,\xi)$.

Figure 16: Third and fourth cumulants of $V_2(t,\xi)$.

The next Figures 17 and 18 present estimates of third joint cumulants and third joint moments of $\big(V_2(t_1,\xi), V_2(t_1,\xi), V_2(t_1+t,\xi)\big)$ and $\big(V_2(t_1,\xi), V_2(t_2,\xi), V_2(t_1+t,\xi)\big)$ respectively, with $t_1 := 35$ms, $t_2 := 45$ms and $t \in [0, 20\text{ms}]$.

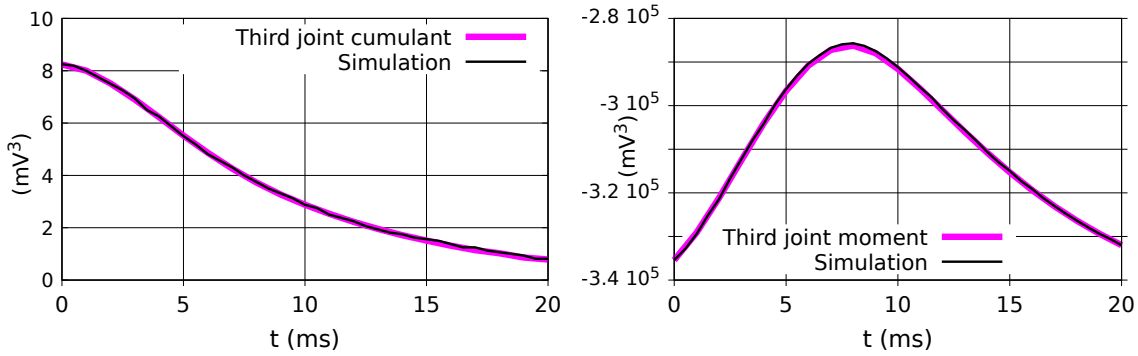

(a) Third joint cumulants. (b) Third joint moments.

Figure 17: Third joint cumulants and moments of $\big(V_2(t_1,\xi), V_2(t_1,\xi), V_2(t_1+t,\xi)\big)$.

The third and fourth cumulant estimates obtained by Monte Carlo simulations with one million samples and above can be subject to numerical instabilities not observed with the closed-form expressions, see Figures 16-a,b), 17-a), 18-a), and Figure 19 below.

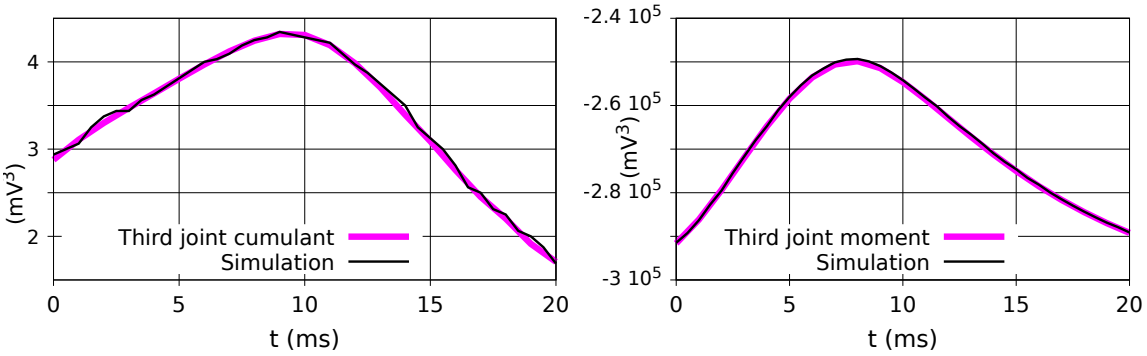

(a) Third joint cumulants. (b) Third joint moments.

Figure 18: Third joint cumulants and moments of $\big(V_2(t_1,\xi), V_2(t_2,\xi), V_2(t_1+t,\xi)\big)$.

Figure 19 presents numerical estimates of skewness $\langle\langle X^3\rangle\rangle/(\langle\langle X^2\rangle\rangle)^{3/2}$ and excess kurtosis $\langle\langle X^4\rangle\rangle/(\langle\langle X^2\rangle\rangle)^2$ of $V_2(t,\xi)$, using the exact expressions (3.2)-(3.4) in the double source model (2.2) of Figure 13. As noted above, the kurtosis estimates obtained in Figure 19 from Monte Carlo simulations are subject to numerical instabilities, and positive skewness/negative excess kurtosis are observed starting after $t = 10$ms.

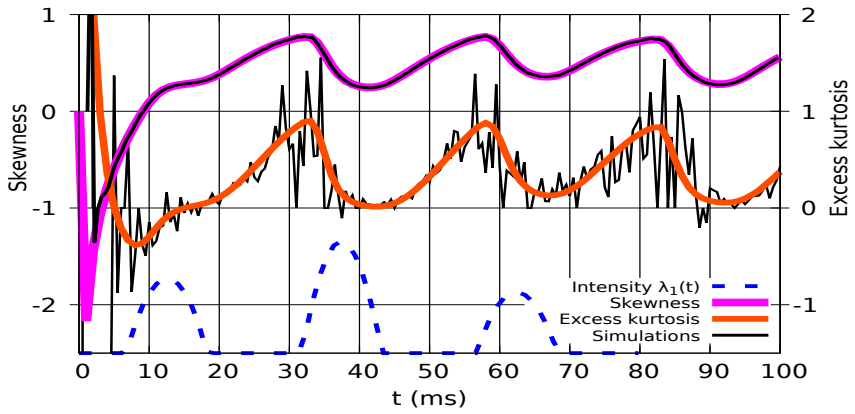

Figure 19: Skewness and excess Kurtosis of $V_2(t, \xi)$.

The next Figure 20 presents the Gram-Charlier density expansions (4.5) based on the exact third and fourth moment expressions (3.3)-(3.4) at different times for the estimation of the probability density function of the membrane potential $V_2(t, \xi)$ in the double source model (2.2) of Figure 13. In comparison with the Gaussian diffusion approximation, the actual probability densities obtained by Monte Carlo simulation have positive skewness, and the best approximations are obtained from fourth-order Gram-Charlier expansions, which appear to correctly fit the purple areas obtained by Monte Carlo simulation of the numerical solution of (2.2). As in Figure 9, the difference between third and fourth-order Gram-Charlier expansion remains minimal, and the biggest differences between actual probability densities and their Gaussian diffusion approximations are observed when skewness and kurtosis take the largest absolute values.

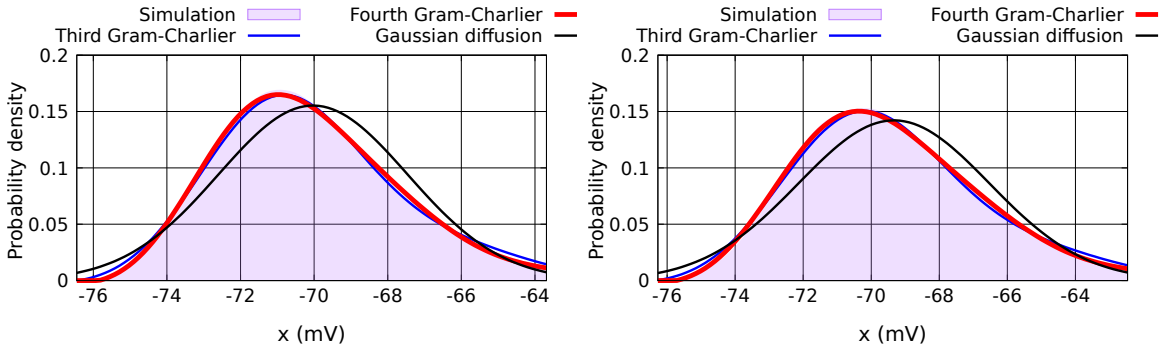

(a) t=30 ms. (b) t=55 ms.

Figure 20: Gram-Charlier density expansions vs simulated densities.

Figure 21 below presents time-dependent fourth-order Gram-Charlier expansions (4.5)

of second and fourth orders based on the exact moment expressions (3.1)-(3.4) at different times, for the probability density function of $V_2(t,\xi)$ in the double source model (2.2) of Figure 13.

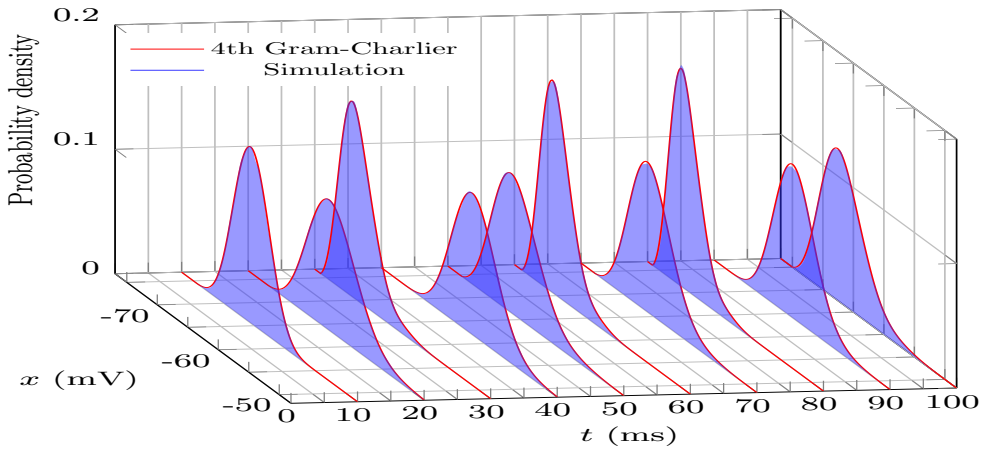

Figure 21: Fourth-order Gram-Charlier expansions vs simulated densities.

Figure 22-a) shows the discrepancies over time between second (blue) and fourth-order (purple) Gram-Charlier expansions for the probability density function of $V_2(t,\xi)$ in the double source model (2.2) of Figure 13, while Figure 22-b) represents the relative difference between the Gaussian diffusion and fourth-order approximations.

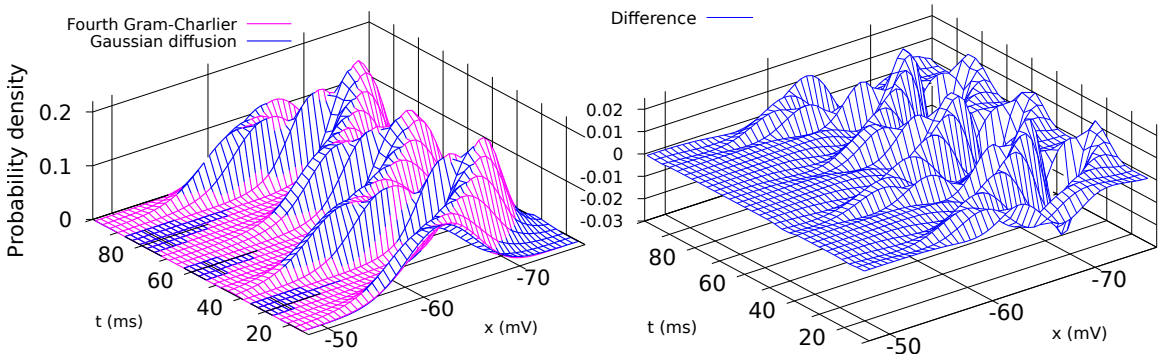

(a) Gaussian diffusion *vs* 4^{th} Edgeworth. (b) Difference between 2^{nd} and 4^{th} Edgeworth.

Figure 22: Fourth-order Gram-Charlier expansions *vs* diffusion approximation.

Impact of leak potentials and intensities on skewness and kurtosis

We consider a double source model of the form (2.1)-(4.10) based on the parameters of Section 2, with $N = 2$, $\mathbb{X} = \mathbb{R}_+ \times [0,2]$, $t_a = 0.01$, $t_b = 0.05$, $\tau = 0.02$s, $\tau_s = 0.0025$s,

$h_e = h_i = 2$, $w_e = 1$, $g_e(u) = g_i(u) = he^{-u/\tau_s}\mathbf{1}_{[0,\infty)}(u)$, $\lambda_e(t) = \lambda_i(t) = \lambda\mathbf{1}_{[t_a,t_b]}(t)$ with $\lambda = 250$Hz, and $\mu(dx, d\theta) = \lambda_e(x)\mathbf{1}_{[0,1]}(\theta)dxd\theta + \lambda_i(x)\mathbf{1}_{[1,2]}(\theta)dxd\theta$. We note that this model coincides with the single source model of Section 4.3 when $w_i = w_e$.

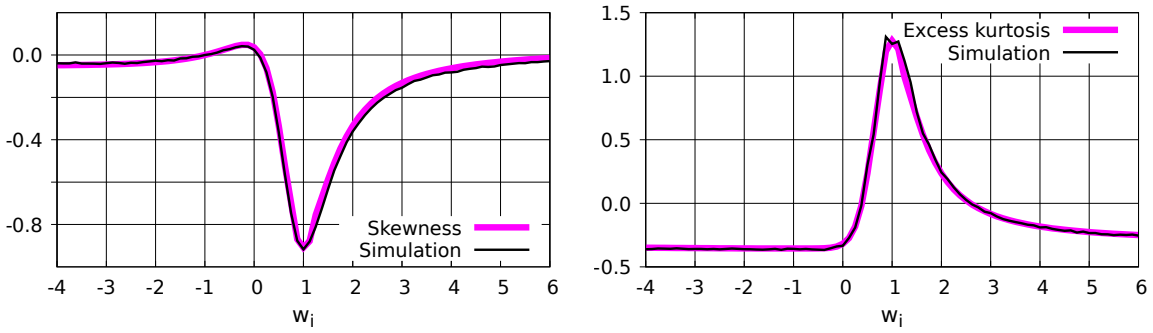

(a) Impact on skewness.

(b) Impact on excess kurtosis.

Figure 23: Skewness and excess kurtosis plots as functions of w_i.

Figure 23 plots the skewness and excess kurtosis of $V_2(t, \xi)$ as functions of the potential w_i, at time $t := 0.03$. We check that skewness and kurtosis evolve in opposite directions, and reach their absolute maxima with negative skewness and positive excess kurtosis when $w_i = w_e$, i.e. in the single source model, cf. Figure 8. The positive skewness and negative excess kurtosis observed in the double source model of Figure 19 can be obtained with positive w_e and negative w_i.

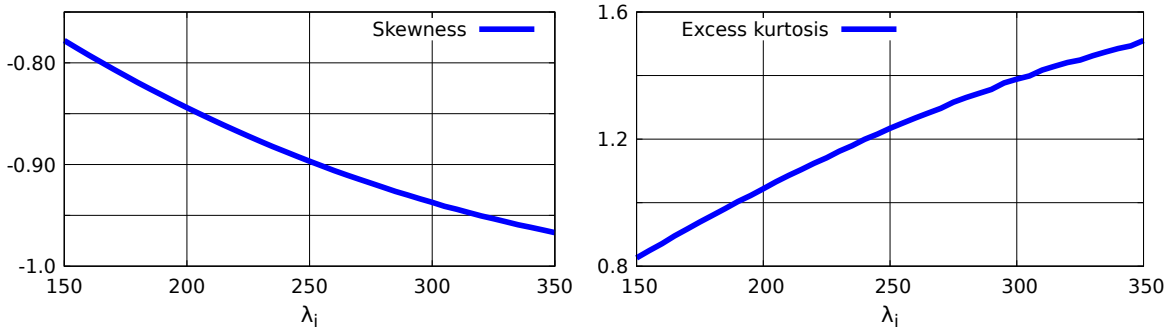

(a) Impact on skewness.

(b) Impact on excess kurtosis.

Figure 24: Skewness and excess kurtosis plots as functions of λ_i.

Figure 24 shows the evolution of the skewness and kurtosis of $V_2(t, \xi)$ in opposite directions as functions of the intensity parameter λ_i when $\lambda_e(t) = \lambda_e\mathbf{1}_{[t_a,t_b]}(t)$ and $\lambda_i(t) = \lambda_i\mathbf{1}_{[t_a,t_b]}(t)$, with $\lambda_e = 250$Hz, $w_e = w_i = 1$, and $t = 0.03$. Here, the impact of λ_e coincides with that of λ_i due to the symmetry of the parameters.

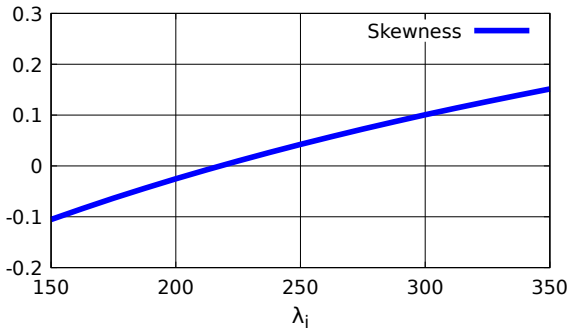

(a) Impact on skewness.

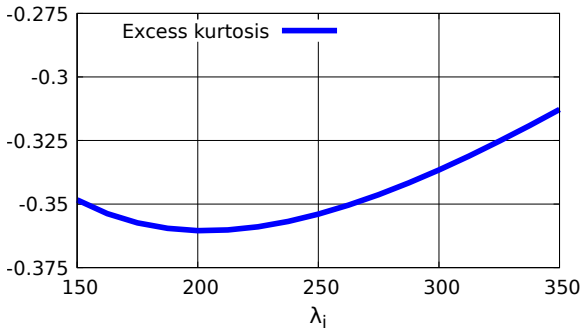

(b) Impact on excess kurtosis.

Figure 25: Skewness and excess kurtosis plots as functions of λ_i with $\lambda_e = 250$Hz.

Figures 25 and 26 show the evolution of the skewness and kurtosis of $V_2(t, \xi)$ as functions of λ_i and λ_e with the biological parameter values $w_e = 1$ and $w_i = -0.25$ at $t = 0.03$.

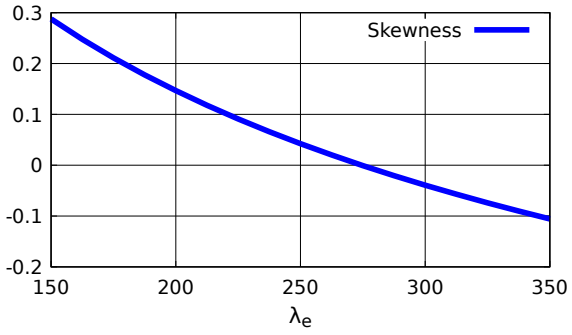

(a) Impact on skewness.

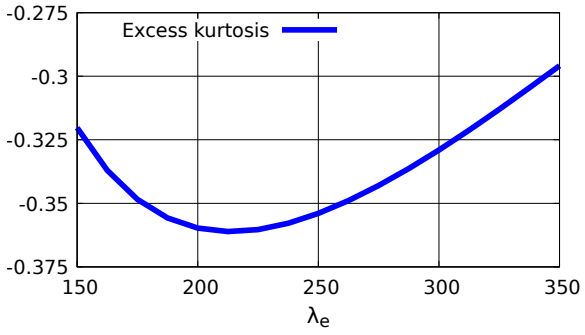

(b) Impact on excess kurtosis.

Figure 26: Skewness and excess kurtosis plots as functions of λ_e with $\lambda_i = 250$Hz.

Conclusion

We investigated the estimation of probability densities of neuronal membrane potentials at fixed times using Gram-Charlier density expansions in nonstationary multiplicative shot noise models with single source and multiple sources. Our method relies on closed-form expressions for moments and cumulants which are numerically more stable than their Monte Carlo simulation counterparts, and shows that the probability density functions of membrane potentials can significantly differ from their continuous Gaussian diffusion approximations. In the nonstationary double source model, positive skewness and negative excess kurtosis of actual probability densities can be

obtained with potentials w_e and w_i of opposite signs. Negative skewness and positive excess kurtosis are observed when $w_e = w_i$ have same positive sign (after identifying corresponding neuron types with such characteristics), and in this setting the skewness and kurtosis of $V_2(t,\xi)$ evolve in opposite directions as functions of λ_i, λ_e.

5 Appendix - moments of Poisson shot noise processes

In this section we apply the results in Privault (2012; 2016) to the derivation of exact expressions for the moments of shot noise stochastic integrals

$$\int_{\mathbb{X}} u(x,\xi)\xi(dx) = \sum_{x_j\in\xi} u(x_j,\xi) \tag{5.1}$$

of random integrands $u(x,\xi)$, with respect to a Poisson point process $\xi(dx)$ with intensity measure $\mu(dx)$ on

$$\Omega := \big\{\xi = \{x_i\}_{i\in I} \subset \mathbb{X} \ : \ \#(A\cap\xi) < \infty \text{ for all compact } A \in \mathcal{B}(\mathbb{X})\big\}$$

of locally finite configurations on a subset $\mathbb{X} \subset \mathbf{R}^d$. In this framework, the moment generating function of the Poisson stochastic integral (5.1) is known to be given by the Lévy-Khintchine formula

$$\left\langle \exp\left(\int_{\mathbb{X}} f(x)\xi(dx)\right)\right\rangle = \exp\left(\int_{\mathbb{X}} (\mathrm{e}^{f(x)}-1)\mu(dx)\right), \tag{5.2}$$

see e.g. Theorem 1.2.14 in Applebaum (2009), provided that f is a sufficiently integrable deterministic function. The moment of order $n \geq 1$ of the Poisson stochastic integral of a deterministic function f can be expressed from (5.2) as

$$\left\langle \left(\sum_{x\in\xi} f(x)\right)^n \right\rangle = n! \sum_{\substack{r_1+2r_2+\cdots+nr_n=n\\ r_1,\ldots,r_n\geq 0}} \prod_{k=1}^{n} \left(\frac{1}{(k!)^{r_k} r_k!} \left(\int_{\mathbb{X}} f^k(x)\mu(dx)\right)^{r_k}\right) \tag{5.3}$$

when $f \in \bigcap_{p=1}^n L^p(\mathbb{X},\mu)$, see Bassan and Bona (1990). For convenience we will use the following notation.

Definition 5.1 *For any $x_1,\ldots,x_k \in \mathbb{X}$, we let $\epsilon^+_{x_1}\cdots\epsilon^+_{x_k}$ denote the operator*

$$(\epsilon^+_{x_1}\cdots\epsilon^+_{x_k}F)(\xi) = F(\xi\cup\{x_1,\ldots,x_k\})$$

acting on random variables F by addition of points at locations $x_1, \ldots, x_k$ to the point process $\xi(dx)$.

The following moment identity, see Theorem 1 in Privault (2016), rewrites the identity (5.3) using sums over partitions $\{\pi_1, \ldots, \pi_k\}$ of $\{1, \ldots, n\}$, and extends it to random integrands $u : \mathbb{X} \times \Omega \longrightarrow \mathbb{R}$. It can be regarded as a nonlinear extension of the Slivnyak-Mecke formula (Slivnyak (1962), Mecke (1967)) which treats the case $n = 1$.

Proposition 5.2 *Let $u : \mathbb{X} \times \Omega \longrightarrow \mathbb{R}$ denote a stochastic process $u(x, \xi)$ indexed by $x \in \mathbb{X}$. For any $n \geq 1$, we have*

$$\left\langle \left(\sum_{x \in \xi} u(x, \xi) \right)^n \right\rangle \tag{5.4}$$
$$= \sum_{k=1}^{n} \sum_{\pi_1 \cup \cdots \cup \pi_k = \{1, \ldots, n\}} \mathbb{E}\left[\int_{\mathbb{X}^k} \epsilon_{x_1}^+ \cdots \epsilon_{x_k}^+ \left(u_{x_1}^{|\pi_1|} \cdots u_{x_k}^{|\pi_k|} \right) \mu(dx_1) \cdots \mu(dx_k) \right],$$

where the power $|\pi_i|$ denotes the cardinality of the subset π_i.

The sum (5.4) runs over all partitions $\pi_1, \ldots, \pi_k$ of $\{1, \ldots, n\}$, and $|\pi_i|$ denote the cardinality of the block π_i, $i = 1, \ldots, k$. This result can be more generally stated as the next joint moment identity for Poisson stochastic integrals with random integrands, cf. Proposition 7 in Privault (2016).

Proposition 5.3 *Let $u_1, \ldots, u_p : \mathbb{X} \times \Omega \longrightarrow \mathbb{R}$ be random processes, $p \geq 1$. For all $n_1, \ldots, n_p \geq 0$ and $n := n_1 + \cdots + n_p$, We have*

$$\left\langle \left(\sum_{x_1 \in \xi} u_1(x_1, \xi) \right)^{n_1} \cdots \left(\sum_{x_p \in \xi} u_p(x_p, \xi) \right)^{n_p} \right\rangle \tag{5.5}$$
$$= \sum_{k=1}^{n} \sum_{\pi_1 \cup \cdots \cup \pi_k = \{1, \ldots, n\}} \mathbb{E}\left[\int_{\mathbb{X}^k} \epsilon_{x_1}^+ \cdots \epsilon_{x_k}^+ \left(\prod_{j=1}^{k} \prod_{i=1}^{p} u_i^{l_{i,j}^n}(x_j, \xi) \right) \mu(\mathrm{d}x_1) \cdots \mu(\mathrm{d}x_k) \right],$$

where the sum runs over all partitions $\pi_1, \ldots, \pi_k$ of $\{1, \ldots, n\}$ and the power $l_{i,j}^n$ is the cardinality

$$l_{i,j}^n := |\pi_j \cap (n_1 + \cdots + n_{i-1}, n_1 + \cdots + n_i]|, \qquad i = 1, \ldots, k, \quad j = 1, \ldots, p.$$

Proof. For the sake of completeness, we provide a short proof of this proposition, based on the recursion applied in Decreusefond and Flint (2014) in the case of point processes. Without loss of generality, we assume that $n_1 = \cdots n_p = 1$ with $n = p$, and we note that for $p = 1$, (5.5) is the Slivnyak-Mecke formula (Slivnyak (1962), Mecke (1967)). Next, we note that

$$\left\langle \sum_{x_1 \in \xi} u_1(x_1, \xi) \cdots \sum_{x_{p+1} \in \xi} u_{p+1}(x_{p+1}, \xi) \right\rangle = \left\langle \prod_{i=1}^{p} \left(\left(\sum_{x_{p+1} \in \xi} u_{p+1}(x_{p+1}, \xi) \right)^{1/p} \sum_{x_i \in \xi} u_i(x_i, \xi) \right) \right\rangle.$$

Hence, by applying (5.5) at the rank $p \geq 1$ to the random sums $\sum_{x_i \in \xi} \left(\sum_{x_{p+1} \in \xi} u_{p+1}(x_{p+1}, \xi) \right)^{1/p} u_i(x_i, \xi)$, $i = 1, \ldots, p$, we find

$$\begin{aligned}
&\left\langle \sum_{x_1 \in \xi} u_1(x_1, \xi) \cdots \sum_{x_{p+1} \in \xi} u_{p+1}(x_{p+1}, \xi) \right\rangle \\
&= \sum_{k=1}^{p} \sum_{\pi_1 \cup \cdots \cup \pi_k = \{1, \ldots, n\}} \mathbb{E}\left[\int_{\mathbb{X}^k} \epsilon^+_{x_1} \cdots \epsilon^+_{x_k} \left(\sum_{x_{p+1} \in \xi} u_{p+1}(x_{p+1}, \xi) \prod_{j=1}^{k} \prod_{i \in \pi_j} u_i(x_j, \xi) \right) \mu(\mathrm{d}x_1) \cdots \mu(\mathrm{d}x_k) \right],
\end{aligned}$$

with, by Definition 5.1,

$$\epsilon^+_{x_1} \cdots \epsilon^+_{x_k} \sum_{x_{p+1} \in \xi} u_{p+1}(x_{p+1}, \xi) = \sum_{x_{p+1} \in \xi} \epsilon^+_{x_1} \cdots \epsilon^+_{x_k} u_{p+1}(x_{p+1}, \xi) + \sum_{l=1}^{k} \epsilon^+_{x_1} \cdots \epsilon^+_{x_k} u_{p+1}(x_l, \xi).$$

Hence, by the Slivnyak-Mecke formula we have

$$\begin{aligned}
&\left\langle \sum_{x_1 \in \xi} u_1(x_1, \xi) \cdots \sum_{x_{p+1} \in \xi} u_{p+1}(x_{p+1}, \xi) \right\rangle \\
&= \sum_{k=1}^{p} \sum_{\pi_1 \cup \cdots \cup \pi_k = \{1, \ldots, p\}} \mathbb{E}\left[\int_{\mathbb{X}^k} \sum_{x_{p+1} \in \xi} \epsilon^+_{x_1} \cdots \epsilon^+_{x_k} \left(u_{p+1}(x_{p+1}, \xi) \prod_{j=1}^{k} \prod_{i \in \pi_j} u_i(x_j, \xi) \right) \mu(\mathrm{d}x_1) \cdots \mu(\mathrm{d}x_k) \right] \\
&+ \sum_{k=1}^{p} \sum_{l=1}^{k} \sum_{\pi_1 \cup \cdots \cup \pi_k = \{1, \ldots, p\}} \mathbb{E}\left[\int_{\mathbb{X}^k} \epsilon^+_{x_1} \cdots \epsilon^+_{x_k} \left(u_{p+1}(x_l, \xi) \prod_{j=1}^{k} \prod_{i \in \pi_j} u_i(x_j, \xi) \right) \mu(\mathrm{d}x_1) \cdots \mu(\mathrm{d}x_k) \right] \\
&= \sum_{k=1}^{p} \sum_{\pi_1 \cup \cdots \cup \pi_k = \{1, \ldots, p\}} \mathbb{E}\left[\int_{\mathbb{X}^{k+1}} \epsilon^+_{x_1} \cdots \epsilon^+_{x_{k+1}} \left(u_{p+1}(x_{k+1}, \xi) \prod_{j=1}^{k} \prod_{i \in \pi_j} u_i(x_j, \xi) \right) \mu(\mathrm{d}x_1) \cdots \mu(\mathrm{d}x_{k+1}) \right] \\
&+ \sum_{k=1}^{p} \sum_{l=1}^{k} \sum_{\pi_1 \cup \cdots \cup \pi_k = \{1, \ldots, p\}} \mathbb{E}\left[\int_{\mathbb{X}^k} \epsilon^+_{x_1} \cdots \epsilon^+_{x_k} \left(u_{p+1}(x_l, \xi) \prod_{j=1}^{k} \prod_{i \in \pi_j} u_i(x_j, \xi) \right) \mu(\mathrm{d}x_1) \cdots \mu(\mathrm{d}x_k) \right],
\end{aligned}$$

and we conclude to (5.5) by a rearrangement of the sum over partitions $\pi_1, \ldots, \pi_k$ of $\{1, \ldots, p+1\}$, see e.g. Lemma 3.1 in Decreusefond and Flint (2014). □

The next joint moment identity is a particular case of Proposition 5.3.

Corollary 5.4 *Let $f_1, \ldots, f_p : \mathbb{X} \longrightarrow \mathbb{R}$ be deterministic functions, $p \geq 1$. For any bounded random variable F and $n_1, \ldots, n_p \geq 0$ and $n := n_1 + \cdots + n_p$, we have*

$$\begin{aligned}
&\left\langle F \left(\sum_{x_1 \in \xi} f_1(x_1) \right)^{n_1} \cdots \left(\sum_{x_p \in \xi} f_p(x_p) \right)^{n_p} \right\rangle \\
&= \sum_{k=1}^{n} \sum_{\pi_1 \cup \cdots \cup \pi_k = \{1,\ldots,n\}} \int_{\mathbb{X}^k} \mathbb{E}\left[\epsilon^+_{x_1} \cdots \epsilon^+_{x_k} F \right] \prod_{j=1}^{k} \prod_{i=1}^{p} f_i^{l^n_{i,j}}(x_j) \mu(\mathrm{d}x_1) \cdots \mu(\mathrm{d}x_k).
\end{aligned}$$

If $n_1 = \cdots = n_p = 1$ we have $n = p$, and

$$\begin{aligned}
&\left\langle F \sum_{x_1 \in \xi} f_1(x_1) \cdots \sum_{x_p \in \xi} f_p(x_p) \right\rangle \qquad (5.6) \\
&= \sum_{k=1}^{n} \sum_{\pi_1 \cup \cdots \cup \pi_k = \{1,\ldots,n\}} \int_{\mathbb{X}^k} \mathbb{E}\left[\epsilon^+_{x_1} \cdots \epsilon^+_{x_k} F \right] \prod_{j=1}^{k} \prod_{i \in \pi_j} f_i(x_j) \mu(\mathrm{d}x_1) \cdots \mu(\mathrm{d}x_k).
\end{aligned}$$

When $F = 1$ this identity recovers the standard joint moment-cumulant relationship

$$\left\langle \sum_{x_1 \in \xi} f_1(x_1) \cdots \sum_{x_p \in \xi} f_p(x_p) \right\rangle = \sum_{k=1}^{n} \sum_{\pi_1 \cup \cdots \cup \pi_k = \{1,\ldots,n\}} \int_{\mathbb{X}^k} \prod_{j=1}^{k} \prod_{i \in \pi_j} f_i(x_j) \mu(\mathrm{d}x_1) \cdots \mu(\mathrm{d}x_k),$$

see Relation (4.2). The next consequence of Proposition 5.3 will be used to compute the joint moments of shot noise processes in Proposition 5.6.

Corollary 5.5 *Let $f_1, \ldots, f_p, g : \mathbb{X} \longrightarrow \mathbb{R}$ be deterministic functions, $p \geq 1$. We have the joint moment identity*

$$\begin{aligned}
&\left\langle \exp\left(\sum_{x \in \xi} g(x) \right) \sum_{x_1 \in \xi} f_1(x_1) \cdots \sum_{x_p \in \xi} f_p(x_p) \right\rangle \\
&= \mathbb{E}\left[\exp\left(\sum_{x \in \xi} g(x) \right) \right] \sum_{k=1}^{n} \sum_{\pi_1 \cup \cdots \cup \pi_k = \{1,\ldots,n\}} \prod_{j=1}^{k} \int_{\mathbb{X}} \mathrm{e}^{g(x)} \prod_{i \in \pi_j} f_i(x) \mu(\mathrm{d}x).
\end{aligned}$$

Proof. Taking F of the form $F = \exp\left(\sum_{x \in \xi} g(x) \right)$, we have the product expression

$$\epsilon^+_{x_1} \cdots \epsilon^+_{x_k} F(\xi) = \exp\left(\sum_{x \in \xi} g(x) \right) \prod_{l=1}^{k} \mathrm{e}^{g(x_l)}$$

hence by (5.6), we find

$$\begin{aligned}
&\left\langle \exp\left(\sum_{x\in\xi} g(x)\right) \sum_{x_1\in\xi} f_1(x_1)\cdots\sum_{x_p\in\xi} f_p(x_p)\right\rangle \\
&= \sum_{k=1}^{n} \sum_{\pi_1\cup\cdots\cup\pi_k=\{1,\ldots,n\}} \int_{\mathbb{X}^k} \mathbb{E}\left[\epsilon^+_{x_1}\cdots\epsilon^+_{x_k}\exp\left(\sum_{x\in\xi} g(x)\right)\right] \prod_{j=1}^{k}\prod_{i\in\pi_j} f_i(x_j)\mu(\mathrm{d}x_1)\cdots\mu(\mathrm{d}x_k) \\
&= \left\langle \exp\left(\sum_{x\in\xi} g(x)\right)\right\rangle \sum_{k=1}^{n} \sum_{\pi_1\cup\cdots\cup\pi_k=\{1,\ldots,n\}} \int_{\mathbb{X}^k} \prod_{j=1}^{k}\left(\mathrm{e}^{g(x_j)}\prod_{i\in\pi_j} f_i(x_j)\right)\mu(\mathrm{d}x_1)\cdots\mu(\mathrm{d}x_k) \\
&= \left\langle \exp\left(\sum_{x\in\xi} g(x)\right)\right\rangle \sum_{k=1}^{n} \sum_{\pi_1\cup\cdots\cup\pi_k=\{1,\ldots,n\}} \prod_{j=1}^{k}\int_{\mathbb{X}} \mathrm{e}^{g(x)}\prod_{i\in\pi_j} f_i(x)\mu(\mathrm{d}x).
\end{aligned}$$

□

In particular, when F is a random variable and f is a deterministic function, we find

$$\begin{aligned}
&\mathbb{E}\left[F(\xi)\left(\sum_{x\in\xi} f(x)\right)^n\right] \\
&\quad= \sum_{k=1}^{n} \sum_{\pi_1\cup\cdots\cup\pi_k=\{1,\ldots,n\}} \int_{\mathbb{X}^k} f^{|\pi_1|}(x_1)\cdots f^{|\pi_k|}(x_k)\,\mathbb{E}\left[\epsilon^+_{x_1}\cdots\epsilon^+_{x_k}F\right]\mu(dx_1)\cdots\mu(dx_k).
\end{aligned}$$

In Proposition 5.6 we provide the proof of the expression (2.6) of $m_{n,N}(z_1,\ldots,z_n;t_1,\ldots,t_n)$ used in the exact third and fourth moment expressions (3.3)-(3.4).

Proposition 5.6 *For all* $(z_1,\ldots,z_n)\in(-\infty,t_1]\times\cdots\times(-\infty,t_n]$ *we have*

$$\begin{aligned}
&m_{n,N}(z_1,\ldots,z_n;t_1,\ldots,t_n) \\
&= \left\langle \mathrm{e}^{-\frac{1}{\tau}\sum_{l=1}^{n}\int_{z_l}^{t_l} Q_0(u,\xi)du}\right\rangle \sum_{\pi\in\Pi[n]}\prod_{j=1}^{|\pi|}\int_{(-\infty,\hat{z}_{\pi_j}]\times S}\prod_{l=1}^{n}\mathrm{e}^{-\frac{1}{\tau}\int_{z_l}^{t_l} f(u-y,\eta)du}\prod_{i\in\pi_j} f^{(w)}(z_i-y,\eta)\mu(\mathrm{d}y,\mathrm{d}\eta)
\end{aligned}$$

with $\hat{z}_{\pi_j}=\min_{i\in\pi_j} z_i$, *and* $\left\langle \mathrm{e}^{-\frac{1}{\tau}\sum_{l=1}^{n}\int_{z_l}^{t_l} Q_0(u,\xi)du}\right\rangle$ *is given by the Lévy-Khintchine formula* (2.7).

Proof. By Corollary 5.5, we have

$$\left\langle \prod_{k=1}^{n}\left(\mathrm{e}^{-\frac{1}{\tau}\int_{z_k}^{t_k} Q_0(u,\xi)du}\int_{(-\infty,z_k]\times S} f^{(w)}(z_k-u,\theta)\xi(du,d\theta)\right)\right\rangle$$

$$= \sum_{\pi\in\Pi[n]} \int_{((-\infty,t]\times S)^{|\pi|}} \left\langle \epsilon^+_{(y_1,\eta_1)} \cdots \epsilon^+_{(y_{|\pi|},\eta_{|\pi|})} \mathrm{e}^{-\frac{1}{\tau}\sum_{l=1}^n \int_{z_l}^{t_l} Q_0(u,\xi)du} \right\rangle \prod_{j=1}^{|\pi|} \prod_{i\in\pi_j} f^{(w)}(z_i - y_j, \eta_j) \prod_{j=1}^{|\pi|} \mu(\mathrm{d}y_j, \mathrm{d}\eta_j). \tag{5.7}$$

On the other hand, using the notation $\epsilon^+_{(y_1,\eta_1)} \cdots \epsilon^+_{(y_k,\eta_k)}$ introduced in Definition 5.1, we find

$$\begin{aligned}
&\epsilon^+_{(y_1,\eta_1)} \cdots \epsilon^+_{(y_k,\eta_k)} \exp\left(-\frac{1}{\tau}\sum_{l=1}^n \int_{z_l}^{t_l} Q_0(u,\xi)du \right) \\
&= \epsilon^+_{(y_1,\eta_1)} \cdots \epsilon^+_{(y_k,\eta_k)} \exp\left(-\frac{1}{\tau}\sum_{l=1}^n \int_{z_l}^{t_l} \left(1 + \int_{(-\infty,u]\times S} f(u-y,\eta)\xi(dy,d\eta)\right)du \right) \\
&= \exp\left(-\frac{1}{\tau}\sum_{l=1}^n \int_{z_l}^{t_l} \left(1 + \int_{(-\infty,u]\times S} f(u-y,\eta)\xi(dy,d\eta)\right)du - \frac{1}{\tau}\sum_{j=1}^k \sum_{l=1}^n \int_{z_l}^{t_l} f(u-y_j,\eta_j)du \right) \\
&= \mathrm{e}^{-\frac{1}{\tau}\sum_{l=1}^n \int_{z_l}^{t_l} Q_0(u,\xi)du} \prod_{j=1}^k \mathrm{e}^{-\frac{1}{\tau}\sum_{l=1}^n \int_{z_l}^{t_l} f(u-y_j,\eta_j)du},
\end{aligned}$$

hence

$$\left\langle \epsilon^+_{(y_1,\eta_1)} \cdots \epsilon^+_{(y_{|\pi|},\eta_{|\pi|})} \mathrm{e}^{-\frac{1}{\tau}\sum_{l=1}^n \int_{z_l}^{t_l} Q_0(u,\xi)du} \right\rangle = \left\langle \mathrm{e}^{-\frac{1}{\tau}\sum_{l=1}^n \int_{z_l}^{t_l} Q_0(u,\xi)du} \right\rangle \prod_{j=1}^{|\pi|} \mathrm{e}^{-\frac{1}{\tau}\sum_{l=1}^n \int_{z_l}^{t_l} f(u-y_j,\eta_j)du},$$

therefore, by (2.5) and (5.7) we conclude to

$$\begin{aligned}
&m_{n,N}(z_1,\ldots,z_n;t_1,\ldots,t_n) \\
&= \left\langle \prod_{k=1}^n \left(\mathrm{e}^{-\frac{1}{\tau}\int_{z_k}^{t_k} Q_0(u,\xi)du} \int_{(-\infty,z_k]\times S} f^{(w)}(z_k - u,\theta)\xi(du,d\theta) \right) \right\rangle \\
&= \left\langle \mathrm{e}^{-\frac{1}{\tau}\sum_{l=1}^n \int_{z_l}^{t_l} Q_0(u,\xi)du} \right\rangle \\
&\quad \times \sum_{\pi\in\Pi[n]} \int_{((-\infty,t]\times S)^{|\pi|}} \prod_{j=1}^{|\pi|} \left(\mathrm{e}^{-\frac{1}{\tau}\sum_{l=1}^n \int_{z_l}^{t_l} f(u-y_j,\eta_j)du} \prod_{i\in\pi_j} f^{(w)}(z_i - y_j,\eta_j) \right) \prod_{j=1}^{|\pi|} \mu(\mathrm{d}y_j,\mathrm{d}\eta_j) \\
&= \left\langle \mathrm{e}^{-\sum_{l=1}^n \int_{z_l}^{t_l} Q_0(u,\xi)du} \right\rangle \sum_{\pi\in\Pi[n]} \prod_{j=1}^{|\pi|} \int_{(-\infty,\hat{z}_{\pi_j}]\times S} \prod_{l=1}^n \mathrm{e}^{-\frac{1}{\tau}\int_{z_l}^{t_l} f(u-y,\eta)du} \prod_{i\in\pi_j} f^{(w)}(z_i - y,\eta)\mu(\mathrm{d}y,\mathrm{d}\eta),
\end{aligned}$$

which shows (2.6). □

When $N = 1$, the function $m_{n,1}(z_1,\ldots,z_n;t_1,\ldots,t_n)$ in (2.6) can be written as

$$m_{n,1}(z_1,\ldots,z_n;t_1,\ldots,t_n)$$

$$= w_1^n \mathrm{e}^{-\frac{1}{\tau}\sum_{l=1}^n (t-z_l)} \left\langle \mathrm{e}^{-\frac{1}{\tau}\sum_{l=1}^n \int_{z_l}^{t_l} Q_1(u)du} \prod_{k=1}^n \int_{(-\infty,z_k]\times S} g_1(z_k - y, \eta)\xi(dy, d\eta) \right\rangle$$

$$= w_1^n \mathrm{e}^{-\frac{1}{\tau}\sum_{l=1}^n (t-z_l)} \left\langle \mathrm{e}^{-\frac{1}{\tau}\sum_{l=1}^n \int_{z_l}^{t_l} Q_1(u)du} \right\rangle$$

$$\times \sum_{\pi\in\Pi[n]} \prod_{j=1}^{|\pi|} \int_{(-\infty,t]\times S} \prod_{l=1}^n \mathrm{e}^{-\frac{1}{\tau}\int_{z_l}^{t_l} g_1(u-y,\eta)du} \prod_{i\in\pi_j} g_1(z_i - y, \eta)\mu(\mathrm{d}y, \mathrm{d}\eta),$$

which can be recovered by multiple differentiation of the Lévy-Khintchine formula, as

$$\frac{\partial^n}{\partial z_1 \cdots \partial z_n} \left\langle \mathrm{e}^{-\frac{1}{\tau}\sum_{l=1}^n \int_{z_l}^{t_l} Q_1(u)du} \right\rangle$$

$$= \frac{\partial^n}{\partial z_1 \cdots \partial z_n} \exp\left(\int_{(-\infty,t]\times S} \left(\mathrm{e}^{-\frac{1}{\tau}\sum_{i=1}^n \int_{z_i}^{t_i} g_1(u-x,\theta)du} - 1 \right) \mu(dx, d\theta) \right).$$

References

K.-I. Amemori and S. Ishii. Gaussian process approach to spiking neurons for inhomogeneous Poisson inputs. *Neural Comput.*, 13:2763–2797, 2001.

D. Applebaum. *Lévy processes and stochastic calculus*, volume 116 of *Cambridge Studies in Advanced Mathematics*. Cambridge University Press, Cambridge, second edition, 2009.

B. Bassan and E. Bona. Moments of stochastic processes governed by Poisson random measures. *Comment. Math. Univ. Carolin.*, 31(2):337–343, 1990.

M. Brigham and A. Destexhe. The impact of synaptic conductance inhomogeneities on membrane potential statistics. Preprint, 2015a.

M. Brigham and A. Destexhe. Nonstationary filtered shot-noise processes and applications to neuronal membranes. *Phys. Rev. E*, 91:062102, 2015b.

A. N. Burkitt. A review of the integrate-and-fire neuron model: I. Homogeneous synaptic input. *Biol. Cybernetics*, 95:1–19, 2006a.

A. N. Burkitt. A review of the integrate-and-fire neuron model: II. Inhomogeneous synaptic input and network properties. *Biol. Cybernetics*, 95:97–112, 2006b.

D. Cai, L. Tao, A.V. Rangan, and D. W. McLaughlin. Kinetic theory for neuronal network dynamics. *Comm. Math. Sci.*, 4(1):97–127, 2006.

H. Cramér. *Mathematical methods of statistics*. Princeton University Press, Princeton, NJ, 1946.

L. Decreusefond and I. Flint. Moment formulae for general point processes. *J. Funct. Anal.*, 267: 452–476, 2014.

A. Kuhn, A. Aertsen, and S. Rotter. Neuronal integration of synaptic input in the fluctuation-driven regime. *J. Neurosci.*, 24(10):2345–2356, 2004.

P. Lánský and V. Lánská. Diffusion approximation of the neuronal model with synaptic reversal potentials. *Biol. Cybernetics*, 56:19–26, 1987.

E. Lukacs. Applications of Faà di Bruno's formula in mathematical statistics. *Amer. Math. Monthly.*, 62:340–348, 1955.

P. McCullagh. *Tensor methods in statistics*. Monographs on Statistics and Applied Probability. Chapman & Hall, London, 1987.

J. Mecke. Stationäre zufällige Masse auf lokalkompakten Abelschen Gruppen. *Z. Wahrscheinlichkeitstheorie Verw. Geb.*, 9:36–58, 1967.

N. Privault. Moment identities for Poisson-Skorohod integrals and application to measure invariance. *C. R. Math. Acad. Sci. Paris*, 347:1071–1074, 2009.

N. Privault. Moments of Poisson stochastic integrals with random integrands. *Probability and Mathematical Statistics*, 32(2):227–239, 2012.

N. Privault. Combinatorics of Poisson stochastic integrals with random integrands. In G. Peccati and M. Reitzner, editors, *Stochastic Analysis for Poisson Point Processes: Malliavin Calculus, Wiener-Itô Chaos Expansions and Stochastic Geometry*, volume 7 of *Bocconi & Springer Series*, pages 37–80. Springer, Berlin, 2016.

N. Privault and G.L. Torrisi. Density estimation of functionals of spatial point processes with application to wireless networks. *SIAM J. Math. Anal.*, 43:1311–1344, 2011.

M. Richardson and W. Gerstner. Synaptic shot noise and conductance fluctuations affect the membrane voltage with equal significance. *Neural Comput.*, 17:923–947, 2005.

M. Rudolph and A. Destexhe. An extended analytic expression for the membrane potential distribution of conductance-based synaptic noise. *Neural Comput.*, 17:2301, 2005.

I.M. Slivnyak. Some properties of stationary flows of homogeneous random events. *Theory Probab. Appl.*, 7(3):336–341, 1962.

H.C. Tuckwell. *Introduction to Theoretical Neurobiology: Volume 2, Nonlinear and Stochastic Theories*. Cambridge University Press, Cambridge, 1988.

A. Verveen and L. DeFelice. Membrane noise. *Progress in Biophysics and Molecular Biology*, 28: 189–234, 1974.

L. Wolff and B. Lindner. Method to calculate the moments of the membrane voltage in a model neuron driven by multiplicative filtered shot noise. *Phys. Rev. E*, 77:041913, 2008.

L. Wolff and B. Lindner. Mean, variance, and autocorrelation of subthreshold potential fluctuations driven by filtered conductance shot noise. *Neural Comput.*, 22:94–120, 2010.